Unstable Thin Film Spreading of Volatile Binary Mixtures

Teemu Isojärvi

Master's Thesis November 28, 2013
Department of Physics
University of Jyväskylä

Abstract

This Thesis discusses the fluid mechanics of thin films, with emphasis on dynamical instabilities observed in some situations. The theoretical part first presents the main theory of thin-film flow, and then advances to discuss the problems associated with incorporation of evaporative effects and binary mixtures in the model. In the experimental part, measurements related to spreading of certain class of binary mixtures are presented. The studied mixtures have a volatile component with low surface tension and a less volatile component with high surface tension. The main example of such a mixture is the water-isopropanol system.

Contents

Chapter 1

Introduction

The physics of thin liquid films is a branch of fluid mechanics that is highly interesting considering both applications and theory. Thin films appear in a variety of industrial processes, such as the spin-coating method used in fabrication of microelectronics [1]. Another emerging application is in the field of self-organized nanostructures [2].

From the theoretical point of view, the behavior of thin films is an example of nonlinear dynamics. Nonlinear systems are known for exhibiting chaotic, unstable behavior under certain conditions, and such phenomena have long been a subject of intense research interest. A dynamically unstable system is characterized by high sensitivity for external perturbations and changes in initial conditions, and can behave in an essentially unpredictable manner. An example of unstable thin film flow is the "fingering instability", which can occur when a layer of fluid flows down an inclined plane (see Fig. 1.1). In such a situation, the liquid front advances with different speeds at different positions along the three-phase contact line, and it is basically impossible to predict the exact shape that the advancing front assumes. Even in such situations, it is possible to form an equation describing the relation of average finger width to the viscosity and surface tension of the fluid, though.

The structure of this Thesis is as follows: in Chapter 2, the basic equations governing thin film flow and evaporation are described. The experimental Chapters 3 and 4 concentrate on an example of unstable thin-film spreading in the case where the liquid is a mixture of isopropyl alcohol (IPA) and water, or more generally, a mixture of volatile low-surface tension component (component 1) and a less volatile high-surface tension component (component 2).

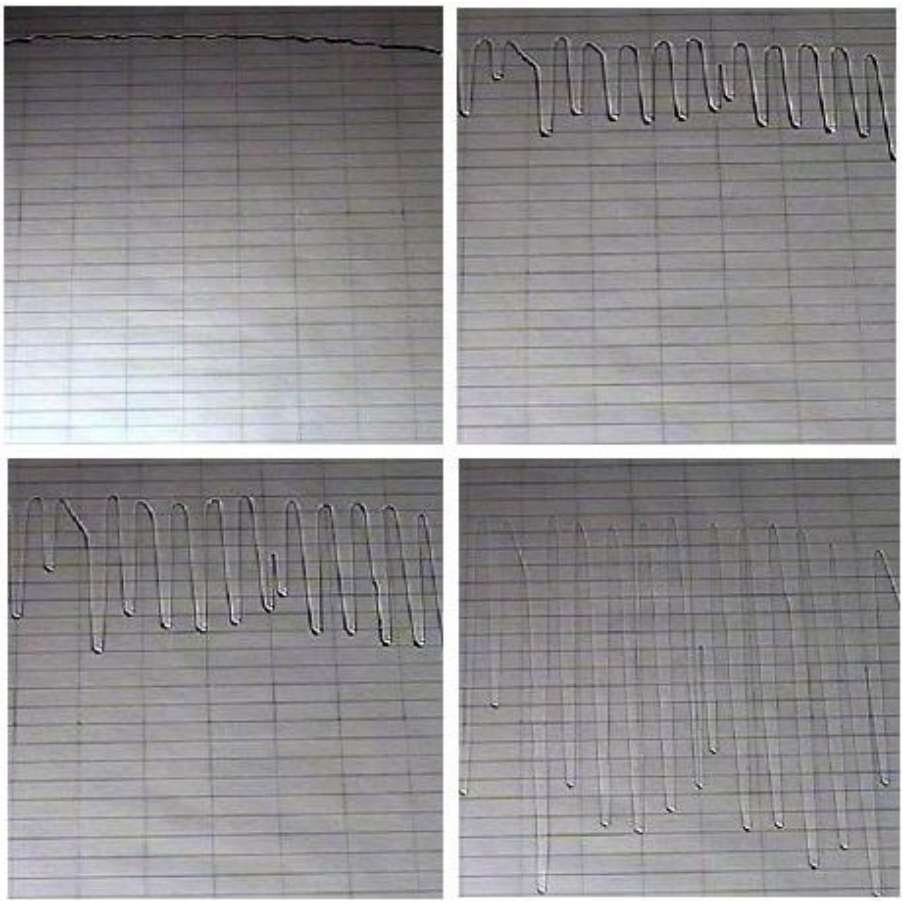

Figure 1.1: Fingering instability in a liquid front flowing down an inclined plane [18]

Chapter 2

Theory of Liquid Films and Drops

When investigating the behavior of a physical system, one usually first finds out how to fully specify a momentary state of the system, and then attempts to form a differential equation which determines the time evolution of the state. For example, the state of a planetary system in Newtonian mechanics is given by specifying the coordinates and momenta of the planets (ignoring internal degrees of freedom, i.e. planetary rotation), and the time evolution is determined by a set of coupled Lagrange equations with pairwise gravitational potential $V_{12} \propto r_{12}^{-1}$. When doing quantum mechanics in the position representation, the state of the quantum system is fully described by some wavefunction Ψ, which evolves according to the time-dependent Schrödinger equation.

The behavior of droplets and thin films is an example of continuum mechanics, where the state of the system is specified by giving the density and velocity fields of the fluid, and hydrodynamical equations determine the time evolution. For viscous flow of an incompressible fluid, the relevant PDE is the Navier-Stokes equation, which is basically a statement of Newton's second law in continuous matter.

In this chapter, we will see that in the case of a thin liquid film, the three dimensional Navier-Stokes equation can be replaced by an approximative two-dimensional equation determining the behavior of film thickness $h(x, y)$.

2.1 Lubrication Approximation

Consider a layer of viscous, incompressible liquid lying on a solid substrate which defines the xy-plane. The fluid has some density ρ and a velocity field $\mathbf{u}(x, y, z)$, and the local thickness of the layer is described by a function $h(x, y)$. The dynamics

of the fluid are determined by the Navier-Stokes equation:

$$\frac{\partial \mathbf{u}}{\partial t} + (\mathbf{u} \cdot \nabla)\mathbf{u} = -\frac{1}{\rho}\nabla p + \frac{\mu}{\rho}\nabla^2 \mathbf{u} \tag{2.1}$$

Here $p(x, y, z)$ is the pressure as a function of position. Eq. (2.1) is nonlinear and is well known to predict chaotic (turbulent) behavior under certain conditions [3].

When the function h is very small at all points, the problem seems to be essentially two-dimensional, and one would expect that some kind of simplification of Eq. (2.1) is possible. More specifically, let us assume that the spread of the liquid film in x and y directions is much larger than its maximum thickness in the z direction, and also that the Reynolds number of the flow is small. Now a simpler equation can be formed as follows.

Because of the assumption of small Reynolds number, the inertial terms in Eq. (2.1) can be ignored. Also, we will define horizontal components of the relevant vectors as follows: $\mathbf{u}_H = (u_x, u_y)$, $\nabla_H = \left(\frac{\partial}{\partial x}, \frac{\partial}{\partial y}\right)$. As the scale of the system is a lot smaller in the z-direction than in the horizontal direction, we can assume that the derivatives with respect to z are a lot larger than the horizontal derivatives: $\frac{\partial^2 \mathbf{u}_H}{\partial z^2} >> \frac{\partial^2 \mathbf{u}_H}{\partial x^2} + \frac{\partial^2 \mathbf{u}_H}{\partial y^2}$, leading to approximation

$$\nabla_H p = \mu \frac{\partial \mathbf{u}_H}{\partial z^2} \tag{2.2}$$

This can be integrated twice, using boundary conditions $\mathbf{u}_H|_{z=0} = 0$ (no-slip condition) and $\frac{\partial \mathbf{u}_H}{\partial z}|_{z=h(x,y)} = 0$ (vanishing shear stess at liquid-gas interface). After integration, we obtain:

$$\mathbf{u}_H = \frac{1}{\mu}\left(\frac{z^2}{2} - hz\right)\nabla_H p. \tag{2.3}$$

Next, we integrate again to find the z-independent average flow velocity $\langle \mathbf{u} \rangle$ at coordinates (x,y):

$$\langle \mathbf{u} \rangle = \frac{1}{h(x,y)} \int_0^{h(x,y)} \mathbf{u} dz = -\frac{h^2}{3\mu}\nabla_H p. \tag{2.4}$$

On physical grounds, one can also require that the continuity equation holds:

$$\frac{\partial h}{\partial t} + \nabla \cdot (h \langle \mathbf{u} \rangle) = 0. \tag{2.5}$$

Combining (2.4) and (2.5), and using the formula for Laplace pressure at the liquid-gas interface ($p - p_{atm} = -\gamma \nabla^2 h$, where p_{atm} is the external atmospheric pressure and γ is the surface tension of the liquid) finally yields the result

$$\frac{\partial h}{\partial t} = -\frac{\gamma}{3\mu}\nabla \cdot (h^3 \nabla(\nabla^2 h)), \tag{2.6}$$

which is the simplest form of the so called *lubrication equation*. More detailed derivations can be found in Refs. [4,5]

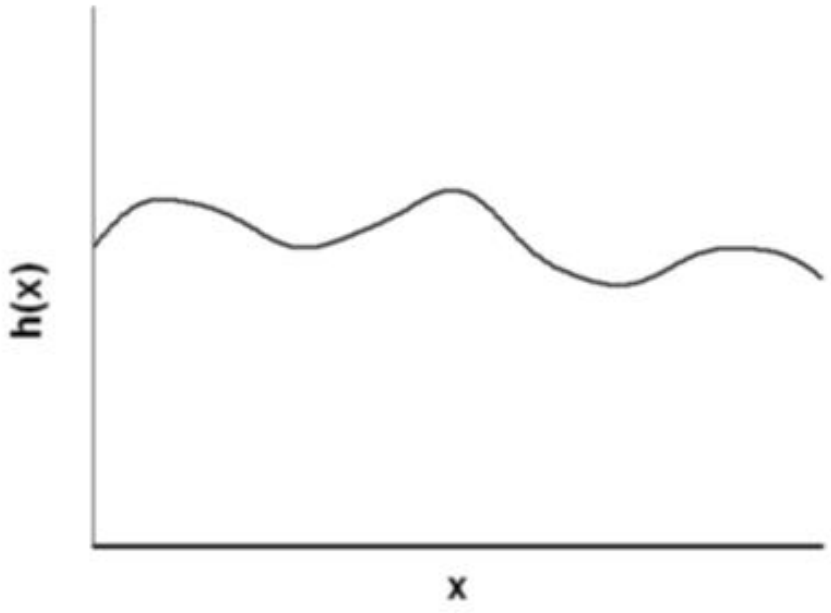

Figure 2.1: The lubrication approximation is valid when the film thickness $h(x)$ is a slowly varying function of position.

Two remarks have to be made about Eq. (2.6). First, the no-slip condition used in obtaining Eq. (2.4) prevents the treatment of moving three-phase contact lines. An attempt to describe such a situation within this model would lead to an unphysical infinite energy dissipation at the advancing liquid front [6]. In these cases the boundary conditions used in obtaining Eq. (2.3) have to be modified to allow for some degree of slip. Second, this model does not take into account the Van der Waals molecular interactions between the liquid and the solid substrate. These interactions become significant when the liquid film is especially thin, and can be modeled by introducing a so called disjoining pressure term in the lubrication equation. These modifications will be discussed in Section 2.2.

The lubrication equation is somewhat unusual, as it is fourth order in the spatial coordinates, while most PDE:s in physics are at most second order. Also, Eq. (2.6) is nonlinear, which immediately hints at the possibility of unstable behavior of the solutions. On the other hand, because the equation is only first order in the time derivative, a knowledge of an initial state $h(x, y, t_0)$ at time t_0 permits the computation of state $h(x, y, t_0 + \Delta t)$ at any later instant $t = t_0 + \Delta t$ by integration.

The lubrication equation has certain nice properties, which are physically obvious requirements. The total volume V of the liquid, $V = \int_{-\infty}^{\infty}\int_{-\infty}^{\infty} h(x,y)dxdy$, is conserved: $\frac{dV}{dt} = 0$. This is easily verified by integrating (2.6) over the whole xy-plane, using the divergence theorem and assuming that the vector quantity $h^3\nabla(\nabla^2 h)$ approaches zero quickly enough when the distance from origin approaches infinity. Another important property is that (2.6) conserves non-negativity of $h(x,y)$. If the initial state $h(x,y)$ is non-negative for all x, y, then the time evolution will keep it such at arbitrary later instants of time.

Next, we will seek static solutions for Eq. (2.6). Here "static" means that the function h is time-independent. Let's ignore gravity and assume that the function h is radially symmetric, depending only on the distance from origin: $h(x,y) = h(r)$. Writing (2.6) in polar coordinates, ignoring angle-dependent terms and setting the time derivative zero, we get the equation

$$\frac{1}{r}\frac{d}{dr}\left[rh^3\left(\frac{d^3h}{dr^3} + \frac{1}{r}\frac{d^2h}{dr^2} + \frac{1}{r^2}\frac{dh}{dr}\right)\right] = 0. \tag{2.7}$$

By guessing or by power series method, one quickly finds out that a solution to (2.7) is $h(r) = a - br^2$, where a and b are positive constants. In other words, in a static situation the liquid surface assumes the shape of a paraboloid of revolution. The function is not bounded from below, but one can form a piecewise defined *weak solution* that is non-negative and solves (2.7) at all points except for one point where it's not differentiable:

$$h(r) = \begin{cases} a - br^2 & : r < \sqrt{\frac{a}{b}} \\ 0 & : r \geq \sqrt{\frac{a}{b}} \end{cases} \tag{2.8}$$

The problem that no nonnegative static strong solution can be found (except for the trivial constant function $h(r) = h_0$) reflects the fact that the simplified lubrication model of Eq. (2.6) does not work at the vicinity of sharp contact lines, where h approaches zero. This will be discussed in Section 2.2.

The prediction of a paraboloid liquid surface at equilibrium seems to be in conflict with the observation that a sessile droplet assumes the shape of a spherical cap in the absence of gravitational effects. This apparent flaw is explained by the fact that a spherical cap is not necessarily very wide compared to its height (as was assumed in the lubrication approximation). If a spherical cap has a large base radius and small height, it can be very accurately approximated with a parabolic surface, so the model is accurate in that limit.

A *similarity solution* to an evolution equation is a solution that only scales as a function of time, while retaining its form. Let us demonstrate this with a familiar PDE, the one-dimensional diffusion equation (this example is chosen because the

lubrication equation itself can be seen as a form of a generalized, nonlinear diffusion equation). The diffusion equation reads

$$\frac{\partial c}{\partial t} = D\frac{\partial^2 c}{\partial x^2}, \tag{2.9}$$

where D is the diffusion constant. Now we seek a solution $c(x,t)$ that fulfills two requirements: first, the integral of $c(x,t)$ over whole x-axis (total mass of solute) stays constant in time, and second, the form of the solution changes only in scale when time advances. From this, and some dimensional analysis, we can deduce that the solution must have the form

$$c(x,t) = \frac{M}{\sqrt{Dt}} f\left(\frac{x}{\sqrt{Dt}}\right), \tag{2.10}$$

Where M is the total mass of the solute. The scaling must be of the form $(Dt)^{-1/2}$ because $\frac{x}{\sqrt{Dt}}$ is the only x-dependent dimensionless variable that can be formed in this situation. Inserting this solution in the diffusion equation and separating variables, we get an ordinary differential equation for the function f:

$$\frac{d^2 f}{dq^2} + \frac{1}{2}\left(f + q\frac{df}{dq}\right) = 0, \tag{2.11}$$

where q=$\frac{x}{\sqrt{Dt}}$. From this equation and the appropriate boundary conditions, one can solve that

$$f(q) = \frac{1}{\sqrt{4\pi}} exp\left(-\frac{q^2}{4}\right), \tag{2.12}$$

and the sought-after similarity solution is

$$c(x,t) = \frac{M}{\sqrt{4\pi Dt}} exp\left(-\frac{x^2}{4Dt}\right). \tag{2.13}$$

In other words, the self-similar solution has a Gaussian form. When a Gaussian initial state $c(x,t_0)$ evolves according to the diffusion equation, it will retain its Gaussian shape at arbitrary later instants of time.

With a similar procedure, one can seek for radially symmetric similarity solutions for the lubrication equation. The form of the solutions is

$$h(r,t) = At^{-\alpha} f(Bt^{-\beta} r), \tag{2.14}$$

where A, B, α, β are some constants and f some function, which can be determined by substituting this trial function in the lubrication equation (an exact analytical solution may be impossible to find, though). It can be shown in this manner that

the base radius of a spreading radially symmetric liquid layer grows proportionally to some root of t, as stated in the *Tanner's spreading law* [7]. Similarity solutions are also useful when studying processes where initially separate droplets coalesce [8].

The lubrication equation, its generalizations, and its properties such as the existence of similarity solutions are also actively studied in the field of pure mathematics. Many mathematical questions related to it still remain unanswered. Examples of purely mathematical papers related to this subject are Refs. [9, 10].

2.2 Improved Lubrication Equations

As mentioned in the previous section, the no-slip condition used in deriving Eq. (2.3) prevents the treatment of moving contact lines, leading to an unphysical stress singularity at the contact line. No-slip condition states that fluid at immediate contact with a solid surface "sticks" to the solid and remains motionless. This condition is very useful when used in its field of applicability, like in modeling the motion of liquid in a cylindrical pipe. Obviously there are situations where it is not applicable because, for example, no conceivable amount of force would be sufficient to sink a solid object in water if the condition would hold in all situations.

The no-slip condition can be relaxed by using a boundary condition

$$\mathbf{u}_H = \kappa(h)\frac{\partial \mathbf{u}_H}{\partial z}, \quad when\ z = 0. \tag{2.15}$$

instead of the no-slip condition $\mathbf{u}_H|_{z=0} = 0$ when obtaining Eq. (2.3) by integration. The function $\kappa(h)$ is called the *slip coefficient*. When using this condition, the resulting version of lubrication equation is given by

$$\frac{\partial h}{\partial t} = -\frac{\gamma}{3\mu}\nabla \cdot \left[\left(h^3 + 3\kappa(h)h^2\right)\nabla(\nabla^2 h)\right]. \tag{2.16}$$

This equation does not have a singularity problem when modeling moving contact lines.

Another thing that was mentioned previously was that Eq. (2.6) does not take into account the Van der Waals interaction between the liquid and substrate, which becomes important at very small film thicknesses. This problem can be resolved by using a modified Laplace pressure (relation between pressure and liquid surface curvature) when deriving the lubrication equation:

$$p - p_{atm} = -\gamma\nabla^2 h + \Pi(h), \tag{2.17}$$

where $\Pi(h)$ is called the disjoining pressure and is generally some function that grows very steeply when h approaches zero. A typical choice for $\Pi(h)$ is

$$\Pi(h) = \frac{A}{h^3}, \tag{2.18}$$

where A is called *Hamaker constant* and can have either a positive or a negative value, depending on the chemical properties of the liquid and the solid. Other forms for the disjoining pressure are also sometimes used, as the exact physics of the liquid-substrate interaction are not yet fully understood. One reasonably realistic form of Π is ([19])

$$\Pi(h) = B\left[\left(\frac{h_*}{h}\right)^n - \left(\frac{h_*}{h}\right)^m\right], \tag{2.19}$$

where h_* is a small positive constant and m, n are also positive constants with $n > m > 1$. For the constant B, it can be shown that

$$B = \frac{(n-1)(m-1)}{h_*(n-m)}\gamma(1 - cos\theta_e), \tag{2.20}$$

where θ_e is the equilibrium liquid-solid contact angle. In other words, this form of disjoining pressure is sophisticated enough to reproduce the experimental fact that all liquid-solid pairs have a characteristic contact angle in a static situation. This is a major improvement to the simple thin film equation, Eq. (2.6), which incorrectly predicts that *any* parabolic liquid surface represents a static situation regardless of contact angle.

With the modified Laplace pressure, the lubrication equation becomes

$$\frac{\partial h}{\partial t} = -\frac{1}{3\mu}\nabla \cdot (h^3 \nabla(\gamma \nabla^2 h - \Pi(h))) \tag{2.21}$$

The problem of moving contact lines can be handled without the slip condition (2.15), if one includes the disjoining pressure term in the lubrication equation, and assumes that instead of reaching zero at the three-phase contact line, the function $h(x, y)$ approaches some very small but nonzero value. In other words, in this model the solid substrate is covered by a microscopically thin *precursor film* of liquid even at points outside the apparent macroscopic contact line. The precursor film model is very commonly used when simulating thin-film dynamics numerically with a computer. The parameter h_* in Eq. (2.19) has an interpretation as the precursor film thickness that has minimum disjoining energy density.

One shortcoming of the simplified lubrication model is that it assumes the liquid film is nonvolatile. Also, the parameters γ, μ are assumed to be constants. When

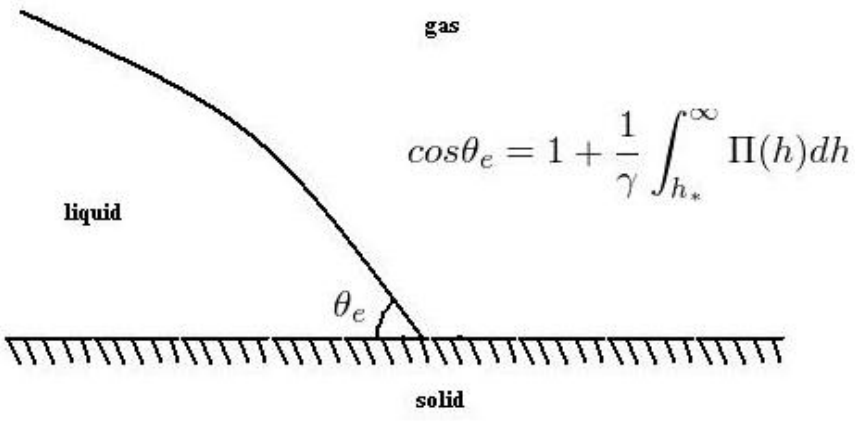

Figure 2.2: Dependence of the equilibrium liquid-solid contact angle on the disjoining pressure function Π is called the Derjaguin formula [20].

a volatile liquid spreads on a surface, evaporative mass loss makes the total liquid volume non-constant, and also different evaporation rates at different points across the liquid surface cause formation of temperature gradients. As surface tension and viscosity are generally temperature-dependent quantities, they will become functions of the space coordinates x, y when the model includes evaporation. These effects can be included by using a following form of modified lubrication equation [11,12]:

$$\frac{\partial h}{\partial t} + \frac{1}{\mu}\nabla \cdot (\frac{h^3}{3}\nabla(\gamma_0 \nabla^2 h) - \gamma_T \frac{h^2}{2}\nabla T) = -\frac{J}{\rho}, \tag{2.22}$$

where $T(x, y)$ is the temperature as a function of position, and the surface tension is assumed to depend linearly on temperature: $\gamma(T) = \gamma_0 + \gamma_T(T - T_0)$. The function $J(x, y)$ is the evaporative mass flux and could in principle be represented as a funtion of $T(x, y)$ and $h(x, y)$.

A problem with this approach is that function $T(x, y)$ in not known beforehand. An exact treatment of the problem would involve solving a system of coupled partial differential equations for the unknown functions T and h. The PDE:s should be constructed to properly describe the evaporative heat loss, and also heat transfer by both conduction and convection. Evaporation rates at different points would have to be solved from a Laplace equation, as will be described in Section 2.5. This problem would be considerably difficult, but there have been attempts to include all these effects in a single equation for $h(x, y)$, as has been done in Refs. [11,12].

Surface tension gradients on a liquid surface are usually termed *Marangoni stresses*, and the tendency of liquid to flow to regions of higher surface tension is called *Marangoni effect*. One well-known phenomenon caused by the Marangoni effect is the so called "tears of wine", where an ethanolic solution flows up a glass surface because of surface tension gradients.

2.3 Instabilities of Liquid Films

A *dynamically unstable system* is characterized by time evolution that is very sensitive to the initial conditions of the system. Two states that are initially seemingly close to each other can evolve to very different states in a relatively short time. Sometimes this leads to chaotic behavior, where the system behaves in a practically indeterministic manner. Such instabilities typically occur when the equations of motion of the system are nonlinear. One example is the turbulence sometimes observed in the solutions of the Navier-Stokes equation.

Consider a one-dimensional version of the lubrication equation, with the disjoining pressure included:

$$\frac{\partial h}{\partial t} = -\frac{1}{3\mu}\frac{\partial}{\partial x}(h^3\frac{\partial}{\partial x}(\gamma\frac{\partial^2 h}{\partial x^2} - \frac{A}{h^3})) \tag{2.23}$$

A static solution of this equation is the constant function $h(x) \equiv h_0$. This function describes a uniform, flat liquid film covering the whole x-axis. The lubrication equation predicts that the time evolution will keep such a state unchanged at any later moment of time. Now we can ask the following question. If the initial state of the liquid film is an "almost constant" function, with a small perturbation added: $h(x, t_0) = h_0 + \epsilon G(x)$, where ϵ is some small number and $G(x)$ some function, will the time evolution keep the film close to a flat film also at later moments in time? If the evolution equation of the system were a linear PDE, this would be the case, but as the lubrication equation is nonlinear, the flat film could represent a state of unstable equilibrium which is broken by the slightest disturbance. A mechanical equivalent of such unstable equilibrium is a ball set exactly on the top of a hemispherical hill.

The stability of the liquid film can be tested with the so-called *linear stability analysis* [13]. Suppose that the perturbation $G(x)$ has the form of a plane wave, and that to first order in the parameter ϵ, its amplitude initially starts either to grow or to decay exponentially:

$$h(x, t) = h_0 + \epsilon e^{\beta t} e^{ikx}. \tag{2.24}$$

If β is positive, the perturbation will grow exponentially and the system is unstable. If it is negative, the system is stable.The parameter β is a bit similar to a Lyapunov

exponent quatifying the stability of a mechanical system, but is not exactly the same thing, as the lubrication equation is not a real equation of motion derived from some Lagrangian.

Substituting the Eq. (2.24) in Eq. (2.23) and discarding terms higher than first order in ϵ, an expression for β can be found in the form:

$$\beta = \frac{Ak^2}{\mu h_0} - \frac{\lambda h_0^3 k^4}{3\mu}. \tag{2.25}$$

From this it can be deduced that if A is negative, the film is always stable. If $A > 0$, the film can be either stable or unstable depending on the parameters k, h_0 and μ. A practical example of an unstable liquid film is a thin layer of water on a hydrophobic solid. The water film easily ruptures and breaks up into drops.

The previous example demonstrated how instabilities are possible in the thin-film dynamics. In addition to instabilities of flat films, there are often situations where the advancing contact line of a spreading film behaves in an unstable manner. Consider a 2-dimensional spreading liquid film with a radially symmetric initial height profile: $h(x, y, t_0) = h(r)$. As the lubrication equations are rotationally invariant, the dynamics should keep the function h symmetric also at later points of time. If h has *compact support*, i.e. is zero outside some finite region, the contact line would have the form of an expanding circle.

Even though the dynamics should conserve rotational symmetry, the nonlinearity of the equations can lead to apparent breaking of that symmetry if there are slightest external perturbations, or deviations of the initial state from exact angle independence. In practice this could mean that the advancing liquid front can form fingers, as mentioned in Chapter 1. The exact fingering pattern which develops can be impossible to predict due to the chaotic nature of the phenomenon. For example, Ref. [12] describes how fingering occurs due to evaporative and gravitational effects in a liquid film flowing down an inclined, inhomogeneously heated plate. There the initial height profile $h(x, y, t_0)$ depends only on one spatial coordinate: $h = h(x)$, where x-axis is the direction of flow. As the lubrication equation is also translation invariant, the function h should remain y-independent at all times. However, because of Marangoni and gravitational effects the system is unstable to perturbations transverse to the direction of flow and fingering occurs. This will be demonstrated in a simulation in Section 2.4

In the experiments carried out in this thesis (Chapters 3 and 4), we describe a contact line instability that takes place when a drop of a concentrated isopropanol solution or other volatile binary mixture spreads on glass surface.In that case, the instability manifests itself as droplet formation at the advancing front of the drop.

2.4 Numerical Simulations

In this section, the process of numerical integration of PDE:s like the lubrication equation is briefly described. For simplicity, we will concentrate on one-dimensional systems. Suppose we have a system where the momentary state at $t = t_0$ is described by a function $f(x, t_0)$, and the time evolution is determined by some (possibly non-linear) partial differential equation, which is of n:th order in the spatial coordinate and of first order in time:

$$\frac{\partial f}{\partial t} = F\left(x, f, \frac{\partial f}{\partial x}, \frac{\partial^2 f}{\partial x^2}, \ldots, \frac{\partial^n f}{\partial x^n}\right). \tag{2.26}$$

An example of such an equation is the one-dimensional diffusion equation, Eq. (2.9). Now we would want to integrate the evolution equation to determine function $f(x, t')$ at some later time $t' > t_0$. To do that with a computer, one first has to choose some finite region of integration (i.e. an interval $[x_1, x_2]$ on the x-axis), large enough that the function f has negligibly small values outside that region in the time interval $[t_0, t']$. Then one can use boundary conditions $f(x_1) = f(x_2) = 0$. Other boundary conditions can also be chosen when appropriate.

Suppose the region of integration is the interval $[0, L]$ on the x-axis. Next we will discretize the time and space intervals. The space interval $[0, L]$ is replaced with a spatial grid with $n_x + 1$ evenly spaced points, spacing $\Delta x = \frac{L}{n_x}$ and the time interval becomes a set of $n_t + 1$ points with spacing $\Delta t = \frac{L}{n_t}$. The function $f(x, t)$ is replaced with a two-index object f^i_j, where the components correspond to values of function f at the grid points:

$$f^i_j \longleftrightarrow f(j\Delta x, i\Delta t). \tag{2.27}$$

Index i can have values $0, 1, 2, \ldots, n_t$ and j can have values $0, 1, 2, \ldots, n_x$.

Derivatives become differences in the discrete system:

$$\frac{\partial f}{\partial x} \longleftrightarrow \frac{f^i_{j+1} - f^i_j}{\Delta x} \qquad \frac{\partial f}{\partial t} \longleftrightarrow \frac{f^{i+1}_j - f^i_j}{\Delta t}. \tag{2.28}$$

Similar expressions can be formed for higher-order derivatives, too. For example:

$$\frac{\partial^2 f}{\partial x^2} \longleftrightarrow \frac{f^i_{j+1} - 2f^i_j + f^i_{j-1}}{(\Delta x)^2}. \tag{2.29}$$

Now, suppose we want to solve a 1-dimensional diffusion problem numerically. We have an initial concentration distribution $c(x, 0)$, and we choose an integration region wide enough that c is very close to zero outside it. Also we choose a spatial resolution

Δx and timestep Δt small enough for the calculation to be accurate. Replacing the partial derivatives in the diffusion equation with corresponding differences, we find that

$$c_j^{i+1} = \frac{D\Delta t}{(\Delta x)^2}\left(c_{j+1}^i - 2c_j^i + c_{j-1}^i\right) + c_j^i. \tag{2.30}$$

Now if we know the initial state $c(x,0) \longleftrightarrow c_j^0$, i.e. we know the numbers $c_1^0, c_2^0, c_3^0, \ldots$, then it would in principle be possible to calculate the state c_j^1 using Eq. (2.28), and then state c_j^2 and so on, advancing a time step of Δt at a time. This kind of direct discretization of the problem is called an *explicit method*.

The problem with this approach is that it is not *numerically stable*. Discretization errors done at consecutive timesteps accumulate, and the total error grows exponentially as a function of t. The correct way to discretize the diffusion equation is the *Crank-Nicolson method* which is described for example in the book "Numerical Recipes in C" [14]. In the Crank-Nicolson scheme, the discrete diffusion equation is

$$-\alpha c_{j+1}^{i+1} + (1+2\alpha)c_j^{i+1} - \alpha c_{j-1}^{i+1} = \alpha c_{j+1}^i + (1-2\alpha)c_j^i + \alpha c_{j-1}^i, \tag{2.31}$$

where $\alpha = \frac{D\Delta t}{2(\Delta x)^2}$. Equation (2.31) describes a tridiagonal system of linear equations that can be used to solve c_j^{i+1} when c_j^i is known. This method is an *implicit method* and can be shown to be numerically stable. In practice, numerical integration of diffusion equation or the time dependent Schrödinger equation is always done with the Crank-Nicolson method.

Next we consider the one-dimensional version of Eq. (2.16), the lubrication equation with slip allowed:

$$\frac{\partial h}{\partial t} = -\frac{\gamma}{3\mu}\frac{\partial}{\partial x}\left[(h^3 + 3\kappa(h)h^2)\frac{\partial^3 h}{\partial x^3}\right]. \tag{2.32}$$

For simplicity, we make this equation dimensionless by setting $\frac{\gamma}{3\mu} = 1$ and we will use the *Navier slip model*, where $3\kappa(h) = \lambda$, where the constant λ is called *slip length*. Of course, the case $\lambda = 0$ corresponds to the no-slip condition.

An attempt to discretize Eq. (2.32) directly with the explicit method leads to numerical instability and blowup of the solution like in the case of the diffusion equation, unless unrealistically large grid sizes are used. One correct way to discretize the lubrication equation is the *explicit-implicit method*, as described by Momoniat *et al.* [15]. With that method, Eq. (2.32) becomes

$$h_j^{i+1} + \alpha_{j+1}^i\left(h_{j+3}^{i+1} - 2h_{j+2}^{i+1} + 2h_j^{i+1} - h_{j-1}^{i+1}\right) - \alpha_{j-1}^i\left(h_{j+1}^{i+1} - 2h_j^{i+1} + 2h_{j-2}^{i+1} - h_{j-3}^{i+1}\right) = h_j^i, \tag{2.33}$$

where

$$\alpha_j^i = \frac{\Delta t}{4\left(\Delta x\right)^4}\left(\left(h_j^i\right)^3 + \lambda\left(h_j^i\right)^2\right). \tag{2.34}$$

As part of this Thesis, a computer program was made for integration of the lubrication equation numerically using Eq. (2.33). The code was written in C++ and a simple Gauss-Jordan elimination routine described in [14] was used to solve the linear system of equations, which occurred at each timestep. In these simulations, the region of integration was chosen to be $x \in [0, 10]$, spatial resolution was $\Delta x = 0.1$ and timestep was $\Delta t = 0.05$. The initial state was chosen to have Gaussian form: $h(x, 0) = exp\left(-\left(x - 5\right)^2\right)$. Two simulations were done, first with slip length $\lambda = 0$ and then with $\lambda = 5$. Convergence was verified by checking that further refinement of the spatial or temporal grid did not notably change the outcome of the simulation. The results of these simulations are shown in Figs. 2.3 and 2.4.

It is evident that when slip length is not zero, the dynamics allow a lot more spreading of the function h than in the no-slip calculation. This is a result of no-slip condition prohibiting any motion of the "contact line", as was described in Section 2.2. Another notable thing about the results is that in the region where h is not very close to zero, the graphs of $h(x)$ approach a parabolic shape as time advances. This can be checked by fitting a second-order polynomial to the computed data points h_j^i.

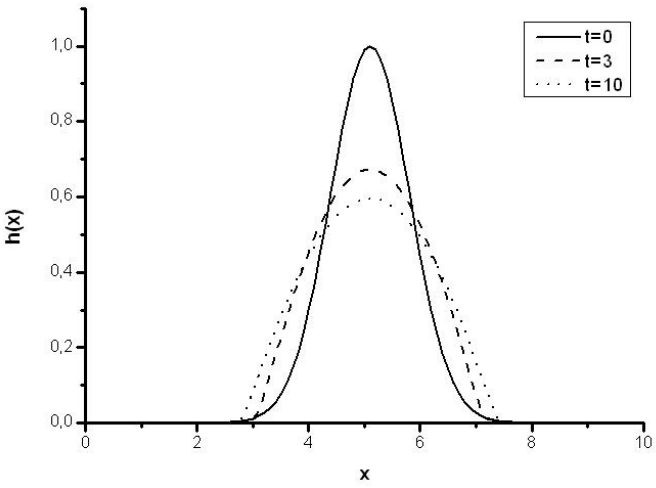

Figure 2.3: Time evolution of a Gaussian initial profile $h(x)$ as determined by the no-slip lubrication equation

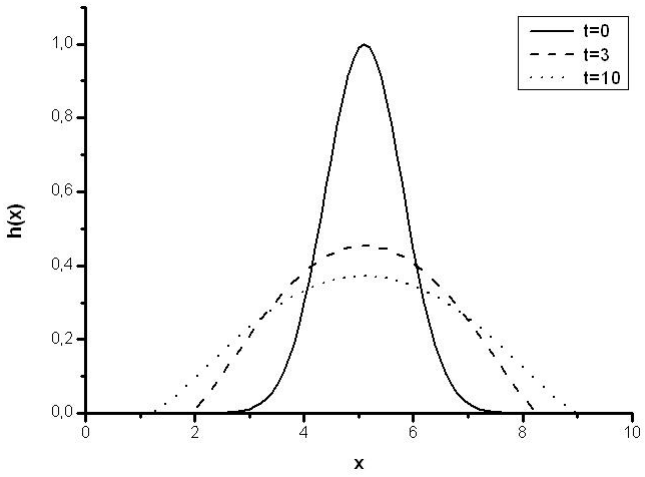

Figure 2.4: Time evolution of a Gaussian initial profile $h(x)$ as determined by the lubrication equation with Navier slip condition

So far the construction of discretized equations has been relatively simple. However, if the thin film equation contains several terms describing different effects, such as the disjoining pressure, finding the correct discretization scheme can become rather tedious. Fortunately, there are commercially available numerical solvers such as COMSOL Multiphysics that use finite-element method to integrate various PDE:s and can be used in numerical simulations with relative ease.

As the first example, consider the thin film equation with a disjoining pressure of the form of Eq.(2.18) (the equation has been made dimensionless by setting $\frac{\lambda}{3\mu} = 1$, this just amounts to choosing the units in which x and t are given):

$$\frac{\partial h}{\partial t} = -\frac{\partial}{\partial x}\left(h^3 \frac{\partial^3 h}{\partial x^3} + \frac{A}{\mu}\frac{1}{h}\frac{\partial h}{\partial x}\right). \tag{2.35}$$

We set the domain of integration to be the interval [0,10] of x-axis and use an initial condition describing an almost flat film with small sinusoidal perturbation added: $h(x,0) = h_0 + \epsilon cos(kx)$. For this simulation, we set $h_0 = 0.2$, $\epsilon = 0.01$, $k = \frac{2\pi}{5}$ and $A/\mu = 0.02$. For the endpoints of the interval, periodic boundary conditions are imposed. The results of the simulation are shown in Fig. 2.5. It is evident that the cosine perturbation starts growing and results in film rupture. This is what can be expected, as plugging the used values of parameters in Eq. (2.25) gives a positive exponent β. If the same simulation is done with a negative value of Hamaker constant, e.g. $A/\mu = -0.02$, it is found that the perturbation starts decaying exponentially instead of growing.

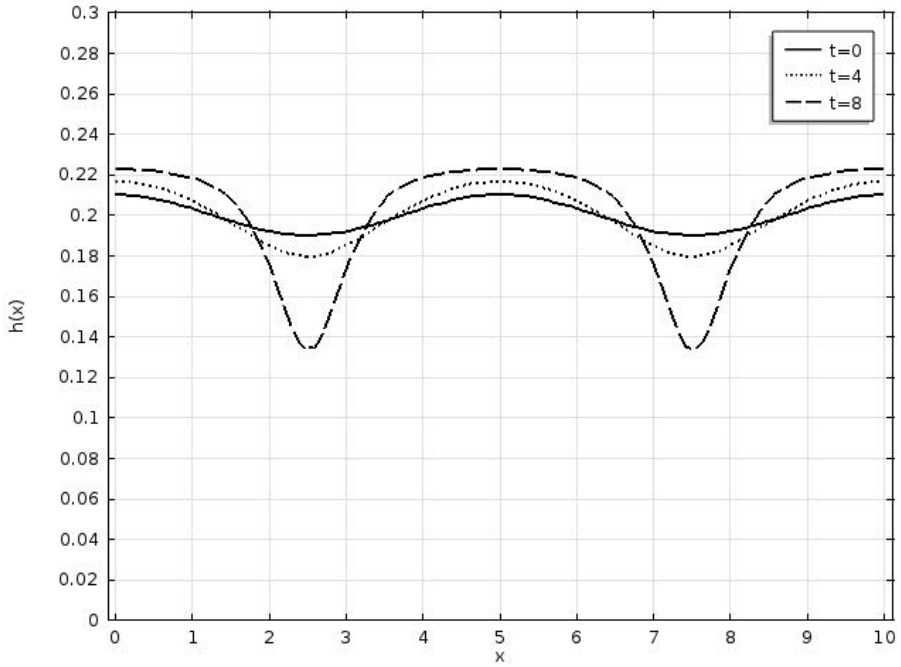

Figure 2.5: Simulation results for a physical situation where a flat liquid film is unstable due to disjoining pressure.

As another example, we study a two-dimensional situation where the contact line becomes unstable. The thin film equation for gravity-driven flow of liquid on an inclined plane is ([18]) given by

$$\frac{\partial h}{\partial t} = -\frac{1}{3\mu}\nabla \cdot \left(\lambda h^3 \nabla \nabla^2 h - \rho g h^3 \nabla h \cos\alpha + \rho g h^3 \sin\alpha \mathbf{i}\right). \tag{2.36}$$

Here α is the angle of inclination, g is the gravitational acceleration and $\mathbf{i}$ is the unit vector in x-direction. For our simulation, we choose the domain of integration to be a rectangle with opposite corners at points $(-8, -24)$ and $(28, 24)$. The values of the parameters are set dimensionless as usual: $\lambda/3\mu = 2$, $\rho g \cos\alpha/3\mu = 2$, $\rho g \sin\alpha/3\mu = 2$. The initial condition is a function of the form:

$$h(x, y, 0) = \frac{1}{2} h_0 \left(1 + \epsilon \cos ky\right) \left(\tanh(-x - x_0) + 1\right). \tag{2.37}$$

This describes a liquid front that has a small cosine form perturbation in the direction transverse to the direction of flow. In this simulation we set $h_0 = 0.2$, $x_0 = 3$, $\epsilon = 0.05$ and $k = \pi/12$. As a boundary condition we require that at the left

boundary of the rectangle, $h(x, y)$ remains constant (i.e. infinite "liquid reservoir" upstream). The results of the simulation are shown in Fig. 2.6.

In the images, one can see that the advancing liquid first forms a thicker capillary ridge (the red/orange area) near the contact line, and then the perturbation is amplified and triangular-shaped fingers form. Perturbations of different wavelengths are not amplified at same rate, and it is possible to form a *dispersion relation* similar to Eq. (2.25), which describes the relation of amplification rate to the wavelength. In this example (flow down an inclined plane), the dispersion relation can't be expressed analytically in closed form except in the limit of long perturbation wavelength [18].

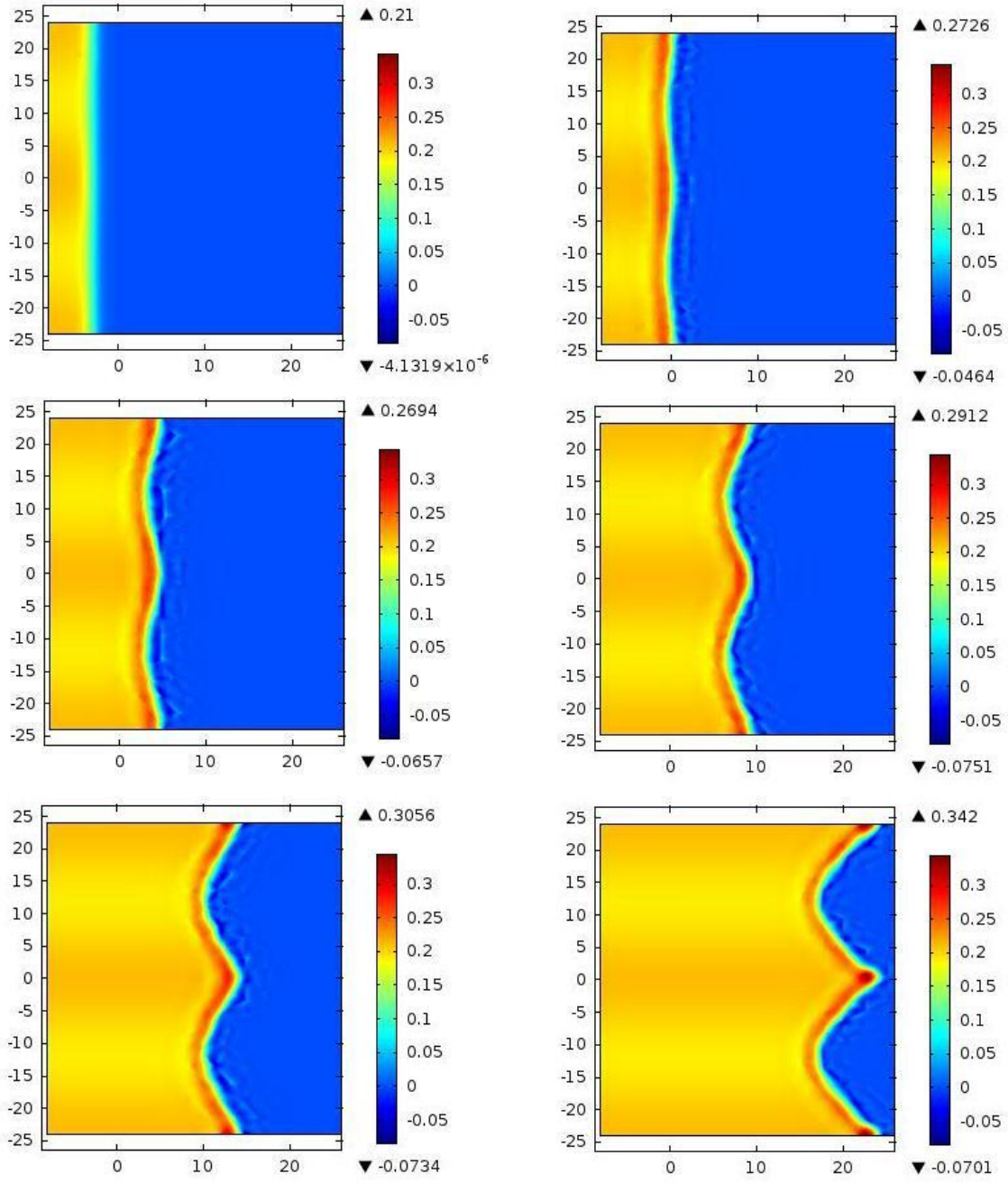

Figure 2.6: COMSOL simulation results demonstrating the fingering instability in gravity-driven thin film flow.

2.5 Evaporation of Liquids

Sometimes a physical problem appears trivial at first glance, but turns out to be very complicated on closer inspection. An example of such a problem is modelling of the evaporation of a sessile drop of water or other liquid on a solid surface. The evaporation rate is observed to depend on the extent of convection in the gas phase above the liquid, and several different evaporation models can be used. The situation is made more complex by complicated evaporatively-induced flows inside the liquid drop.

In a simple model, evaporation is *diffusion limited*. It is assumed that in the immediate vicinity of the liquid surface, the gas phase is saturated with vapor, and the evaporation rate depends on the rate of diffusion of the vapor away from the surface. Such a situation is described by the diffusion equation, Eq. (2.9), where the function $c(x, y, z, t)$ is now the concentration of vapor as a function of position and time. Equation (2.9) can be written in the form

$$\frac{\partial c}{\partial t} = \nabla \cdot \mathbf{j}, \tag{2.38}$$

where $\mathbf{j} = D\nabla c$ is called the *diffusive flux*.

It can be assumed that the evaporation quickly reaches a steady state, where function c is time-independent, but $\mathbf{j}$ is nonzero. In that case, the problem reduces to the Laplace equation:

$$\nabla^2 c = \nabla \cdot \mathbf{j} = 0, \tag{2.39}$$

which is solved with boundary conditions where the function c has some constant limiting value (ambient vapor concentration) far from the liquid surface, and the flux $\mathbf{j}$ vanishes inside the liquid. With the Laplace equation, it is possible to solve the evaporation rates at different points on the surface of the sessile drop in the diffusion-limited regime.

Now a very useful analogy can be noted. The problem is mathematically equivalent with a problem in electrodynamics, where the electric field around a charged conductor is determined. In the diffusion problem, the concentration c is analogous to electric potential ϕ, $\mathbf{j}$ is analogous to electric field $\mathbf{E}$ and the liquid surface replaces the conductor surface (the boundary conditions are same, diffusive flux vanishes inside the liquid, just like $\mathbf{E}$ vanishes inside a conductor).

From electromagnetism, it is known that the electric field near a conductor is highest at point where the curvature of the surface is large, and diverges near sharp edges of the conductor. From this it can be deduced, by analogy, that also the evaporative flux on liquid surface depends on the surface curvature. Also it can be noted that

a sessile drop has a "sharp edge" at the three-phase contact line, therefore the flux $\mathbf{j}$ can be expected to grow very large when approaching the contact line.

Now we could in principle solve the evaporative flux on the surface of a sessile droplet that has the shape of a spherical cap. The problem is analogous to the *electrostatic lens problem*, described in Jackson's *Electrodynamics* [16] and various other sources. It turns out that the exact solution involves special functions, but Deegan *et al.* give a good approximate solution to the problem [17]. If the liquid surface is represented in cylindrical coordinates (r, θ, z), and the base radius of the drop is R, then approximately

$$|\mathbf{j}| \propto \left[1 - \left(\frac{r}{R}\right)^2\right]^{-\lambda}, \tag{2.40}$$

where

$$\lambda = \frac{\pi - 2\theta_c}{2\pi - 2\theta_c} \tag{2.41}$$

and θ_c is the contact angle (angle at which the liquid surface meets the solid). Obviously, the norm of $\mathbf{j}$ has a singularity at the contact line as expected.

The phenomenon of high evaporation near the contact line has a curious consequence when a drop of a colloidal solution evaporates. Inside the drop, there form induced flows that transfer liquid and colloidal particles towards the edges of the drop where most evaporation takes place. As a result, a ring-like deposit of solid precipitate is left on the surface after all liquid has evaporated. This is called *coffee-ring effect*, referring to the ring-like stain that coffee leaves on a table after drying.

2.6 Binary Mixtures

It often happens that liquid materials are not composed of one pure compound, but instead contain two or several different chemical components. A mixture of two components is called a *binary mixture*. If the mixture is volatile, it usually happens that the mole fractions of the components in the vapor are not the same as the fractions in the liquid phase. From basic physical chemistry it can be remembered that a liquid is in equilibrium with its vapor when the chemical potentials μ of all components in the liquid are equal to their chemical potentials in the gas phase. A familiar application of unequal evaporation rates of the liquid components, is purification of materials by distillation.

In the case where the mole fractions are same in liquid and gas at equilibrium, the mixture is called *azeotropic*. Evaporation does not alter the composition of an

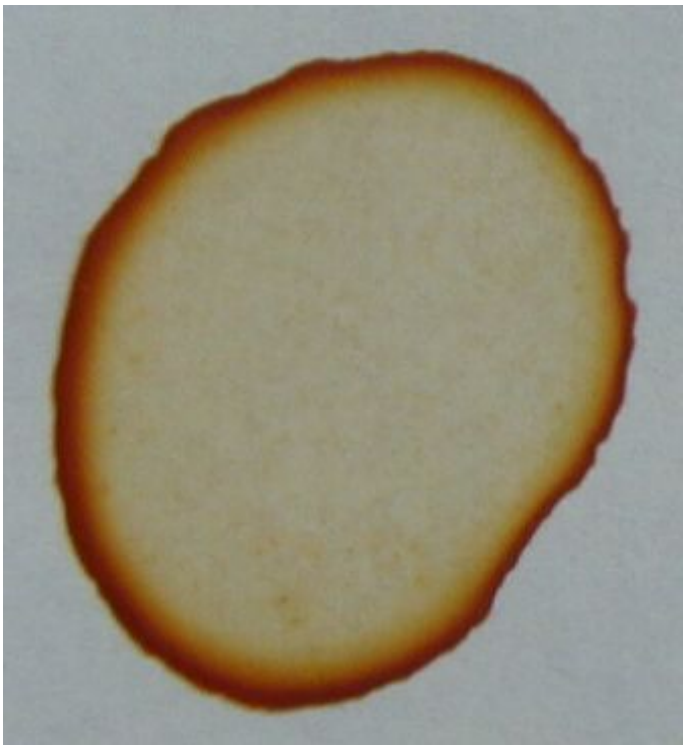

Figure 2.7: Spilled coffee leaves a ring-like stain when it dries, as a result of the differing evaporation rates at different points on a liquid surface.

azeotropic mixture, and it is not possible to concentrate either component by distillation. One example of an azeotrope is a 95.6 mass percent solution of ethyl alcohol in water. Another is 87.4 percent isopropyl alcohol.

Suppose we have a liquid film composed of a volatile, non-azeotropic mixture. Now, as described in previous section, the rate of evaporation is largest near the contact line, at the edges of the film. This will result in a larger concentration of the less volatile component in that region. Usually the surface tension of the mixture depends on the mole fractions, so surface tension gradients (Marangoni stresses) are formed, too. In Section 2.2 it was already described how evaporative effects can make the modeling of liquid film spreading considerably difficult, due to the induced temperature differences. When considering a spreading binary mixture, the problem is even harder, as now a desription of a temporary state of the film would involve three functions: height profile $h(x, y)$, temperature field $T(x, y)$ and mole fraction $\chi(x, y)$ of one component. The coupled PDE:s describing the system would have to take into account transfer of heat and matter by both diffusion and convection.

To the knowledge of the author, no one has yet attempted to form a good theoretical model for the spreading of an evaporating binary mixture. Obviously, a "brute force"-approach, i.e. setting up the coupled equations with all relevant effects included and attempting to integrate them, would not be reasonable. Chapters 3 and 4 describe results of experimental measurements on such systems, and qualitative explanations to the observed phenomena are attempted.

Chapter 3

Experiments with Binary Mixtures

As noted above, the modeling of thin films of evaporating mixtures is difficult because of the need to solve coupled equations taking in account the evaporatively generated gradients in surface tension, viscosity, thermal conductivity, etc. To get a better hold of the problem, experimental work on such systems is necessary. By experimenting with mixtures of various liquids, a qualitative picture can be built on the dependence of the observed phenomena on the physical characteristics of the chemicals.

3.1 Water-Isopropanol system

When a drop of relatively concentrated water solution of isopropyl alcohol (IPA) is dropped on a solid surface, it will immediately begin spreading and forming a thin film, due to its low surface tension. What is interesting about the spreading, is an instability that is observed at the advancing liquid front, or three-phase contact line. Small drops or "beads" of liquid with higher water concentration are observed to form ahead of the expanding contact line. The drops are very small when they are formed, but coalesce and grow progressively larger as the spreading of the film progresses.

This phenomenon can be qualitatively understood to result from the faster evaporation of IPA near the advancing contact line, which results in a larger water concentration and higher surface tension at that region, making formation of droplets possible. Therefore, it is kind of analogous to the coffee ring effect, except that in this case a liquid "ring" is formed instead of a solid deposit ring. This, however, is not the whole picture. A similar instability, nicknamed "octopi", is also seen when 100% anhydrous isopropanol spreads on a silicon or glass surface, as described in

articles by a group in New Jersey Institute of technology, and in a PhD thesis by N.Murisic [21,22]. Therefore, the phenomenon seems to be more complex than one would initially think, and further theoretical and experimental work is necessary to fully understand it.

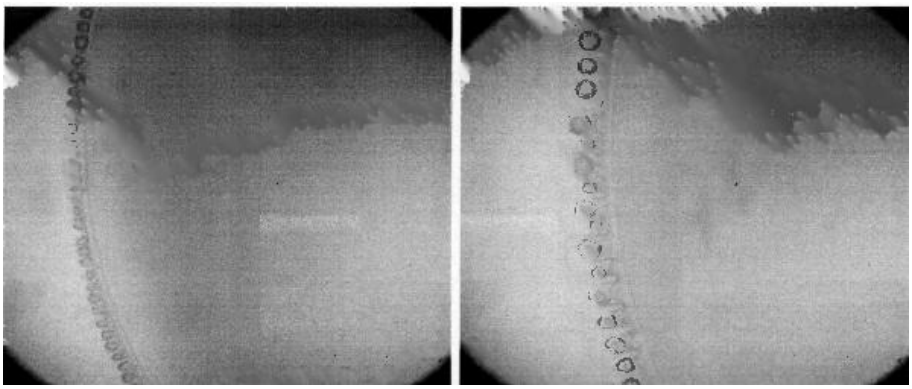

Figure 3.1: Small droplets form at the advancing front of a 70% IPA solution spreading on glass surface

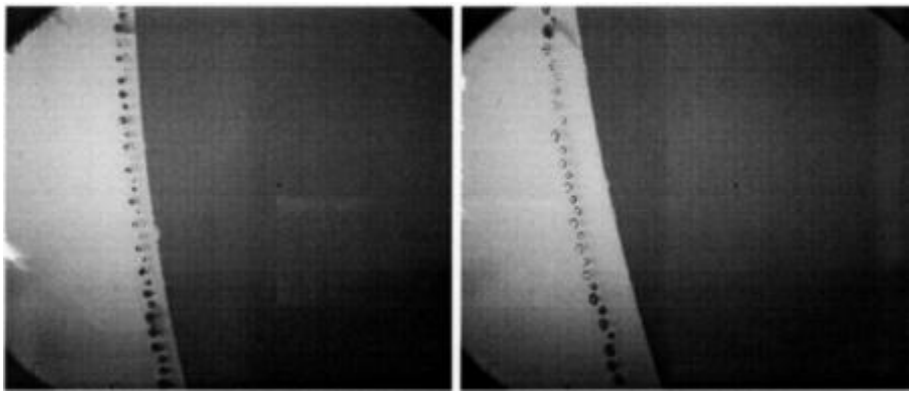

Figure 3.2: When 100% anhydrous IPA spreads on monocrystalline silicon, a different kind of instability is observed and the secondary droplets travel somewhat ahead of the three-phase contact line.

3.2 Mixtures of n-alkanes

Straight-chain alkanes such as n-hexane have surface tensions and volatilities that depend on the length of the carbon chain. Generally, longer chain length results in higher boiling point and slightly higher surface tension. Therefore, mixtures

of different alkanes can be used to investigate the effects of evaporatively induced surface tension gradients on the spreading rates of fully wetting liquids. Tanner's spreading law, which can be derived from the lubrication model, predicts a power-law time dependence for the base radius $R(t)$ of a radially spreading, fully wetting liquid drop: $R(t) \propto t^{\beta}$, where the exponent β has value 1/10 in the case of a non-volatile liquid. Note that by taking the logarithm of the both sides of the power-law equation one gets $log(R(t)) = \beta log(t)$, so by drawing the experimentally measured radii of a spreading drop as a function of time in a log-log plot, one should get a straight line with slope β.

Cazabat *et al.* have investigated the spreading rates and surface profiles of alkane mixture drops of glass surface [23]. The main observation in their work is that a drop of such mixture initially spreads according to the usual Tanner's law with a spreading exponent 1/10, but after a short time, the spreading accelerates and the exponent increases to a value somewhere between 0.2 and 0.3, as shown in Fig. 3.3. A proposed explanation to this behavior is that it takes some time for the concentration gradients to form, after which the outward Marangoni flow increases the spreading rate.

Table 3.1: Physical properties of n-alkanes

Alkane	Surface tension (10^{-3} Nm^{-1})	Boiling point (°C)
Hexane	18.4	68
Heptane	20.5	98
Octane	21.8	125
Nonane	23	150

3.3 Present work

The mixture of isopropanol and water described in Section 3.1 is representative of a more general class of *antagonist mixtures*, which have a volatile component with low surface tension and high wettability (IPA) and a nonvolatile component with high surface tension and low wettability (water). Therefore, there is a motive to research the behavior of other similar mixtures to see how the features of the instability depend on the physical properties of the liquids. Isopropanol could be replaced by some other alcohol (e.g. ethanol) or some other water-soluble volatile solvent, and water could be replaced with the high-boiling-point liquids ethylene glycol or glycerol, both of which have high surface tension and relatively low wettability on glass surface. Physical properties of several suitable liquids are listed in Tables 3.2

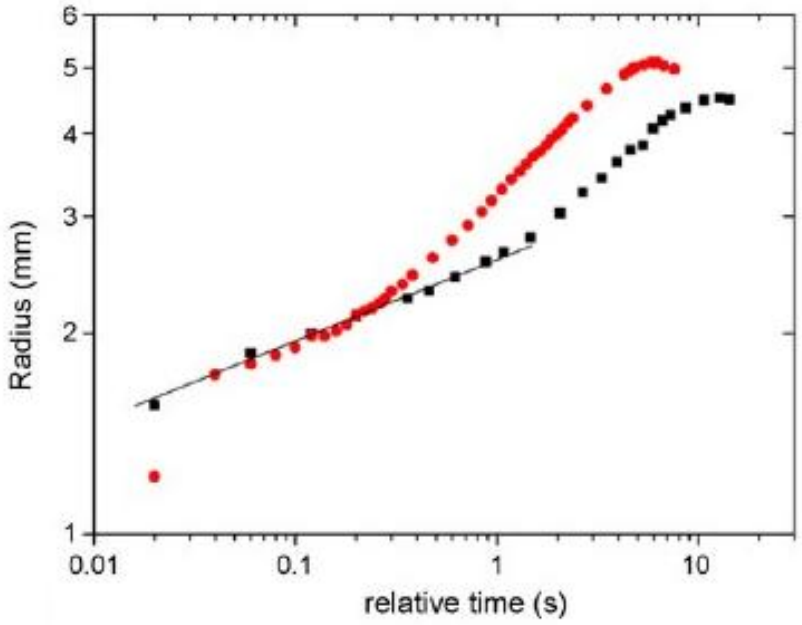

Figure 3.3: Log-log plots of the radii of spreading heptane-octane mixture drops as function of time. The red circles refer to a mixture with 50% heptane and black cubes to a mixture with 10% heptane. The fitted straight line corresponds to simple Tanner's law behavior.

and 3.3.

Some remarks have to be made about the compounds mentioned. Tert-butanol is solid at room temperature, but has a low melting point (26 °C) and also becomes liquid if even a small amount of water is added in it. A crystal of tert-butanol exposed to air will quickly absorb moisture and turns into liquid solution. Diiodomethane (CH_2I_2, bp 182 °C, surface tension 50.88) was initially considered as one high-surface-tension component, but it was found to be not fully soluble in alcohols and the idea was discarded. Other possibility could be formamide ($HCONH_2$, bp 210 °C, surface tension 58.20).

Table 3.2: Properties of several liquids with low boiling point and low surface tension

Compound	Surface tension (10^{-3} Nm^{-1})	Viscosity (cSt)	Boiling point (°C)
Methanol	22.7	0.74	64.7
Ethanol	22.1	1.52	78.4
Isopropanol	23	2.37	82.5
Tert-butanol	solid	solid	82
Acetone	25.2	0.41	56

Table 3.3: Properties of several liquids with high boiling point and high surface tension

Compound	Surface tension (10^{-3} Nm^{-1})	Viscosity (cSt)	Boiling point (°C)
Water	72.8	1.0038	100
Ethylene glycol	47.7	17.8	197
Glycerol	64	648	290
Aniline	43.4	4.37	184

Even though the surface tensions of the volatile alcohols are very similar in value, the surface tensions of their mixtures with water behave differently. The surface tension of a mixture is usually not a weighted average of the surface tensions of individual components, but has a lower value. Generally, adding an alcohol with larger alkyl group in water causes a sharper decrease in surface tension (see Fig. 3.4). This behavior results from the hydrophobic nature of alkyl groups. Obviously this will cause the magnitude of evaporatively formed surface tension gradient to differ in the spreading of droplets of solutions of different alcohols. Similar surface tension data is also available for mixtures such as ethanol-glycol and ethanol-glycerol.

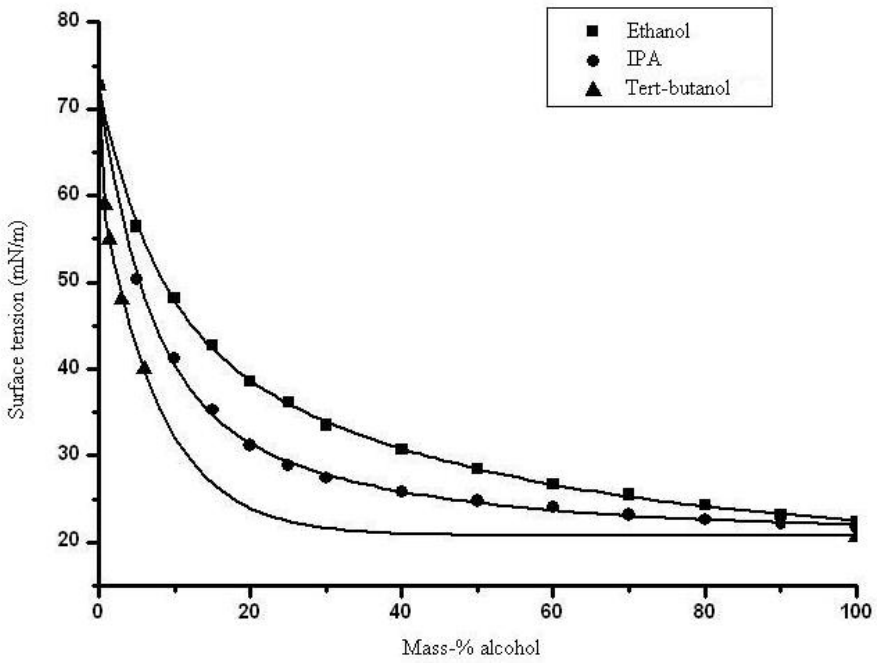

Figure 3.4: The surface tensions (at room temp.) of water solutions of three different alcohols, as a function of the mass percentage of alcohol in the mixture.

The mixtures chosen to be tested in this work were (given in mass-%):

- 70% methanol with 30% water
- 70% ethanol with 30% water
- 70% isopropanol with 30% water
- 60% tert-butanol with 40% water
- 70% isopropanol with 30% ethylene glycol
- 80% isopropanol with 20% glycerol
- 70% isopropanol with 30% aniline

An acetone-water mixture was also preliminarily tested, and it was immediately noted that it did not spread in an unstable manner. The chemicals were obtained from VWR International. The mixtures with correct mass percentages were made using a milligram scale.

The actual measurements were performed by using a syringe, a bent needle and

a micrometer screw to inject microliter-scale drops of the mixtures on glass slides (Mentzel-gläser). The size of the drops was of course not accurately same in different measurements, as the mixures differ in viscosity and surface tension, affecting the size of drops dripping from the needle. The spreading process was observed from above with an experimental setup consisting of a magnifying high-speed camera and mirrors. Images of the spreading liquid film were recorded at constant time intervals.

The camera used in our measurements was of type Redlake Motionpro X3, with maximum resolution of 1024x1280 pixels. With the maximum resolution it was possible to take 1000 images per second (imaging frequency is limited by the large disk space taken by a large number of images, and by the processing speed of the hardware). The width of the imaged area could range from 1 mm to 10 mm. Illumination was provided from below with a panel of 16 high-power LED:s through a diffuser plate.

The grayscale images were processed with ImageJ 1.44p software, and the "blank" background (first image) was subtracted. Also, the colors of the images were inverted and contrast was enhanced to make the images clearer. The images were used to calculate the spreading rates of the different mixtures and to observe qualitative features of the contact-line behavior of the spreading liquid films. The results are shown in Chapter 4.

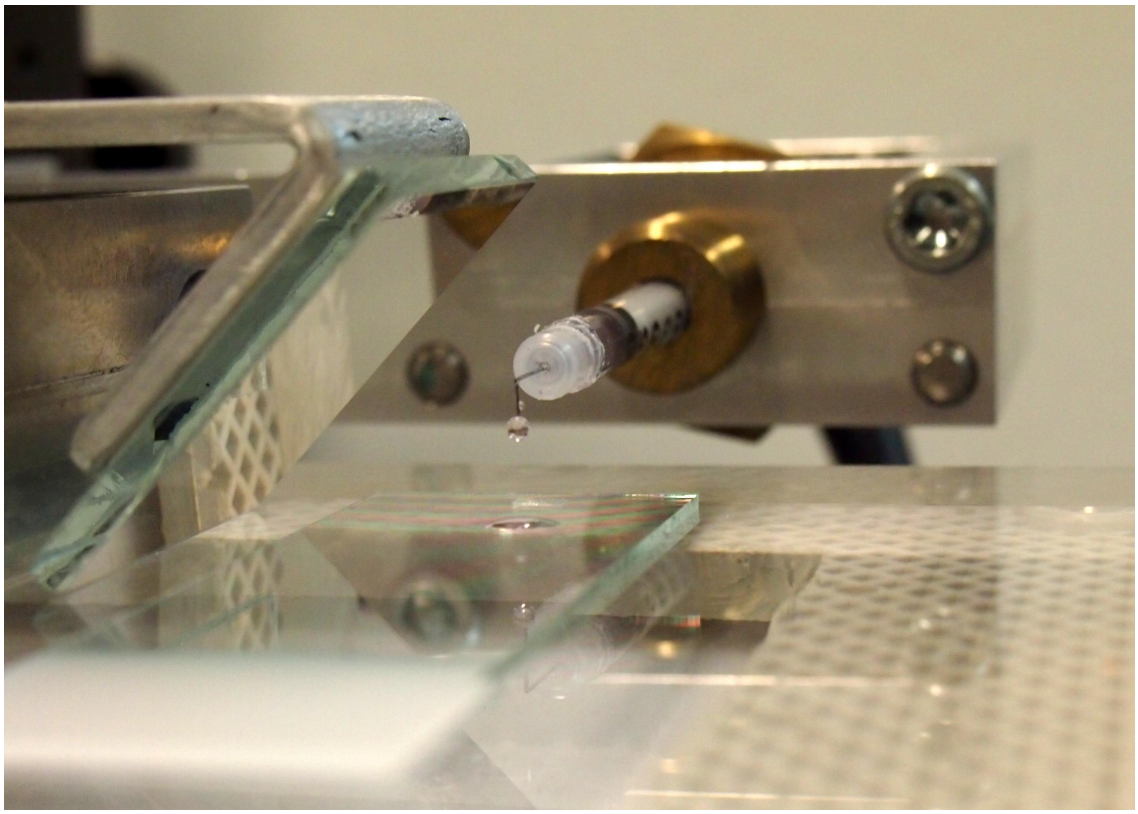

Figure 3.5: An image of the measuring apparatus. Drops of liquid mixtures can be dripped on the glass slide from the syringe and needle, and the high-speed camera on the right (not visible) records the drop spreading process through the mirror in 45° angle.

Chapter 4

Results

4.1 Qualitative features

In the measurements, it was found that almost all of the studied mixtures exhibited unstable contact-line behavior (fingering or droplet formation) in their spreading on glass surface. Exceptions were the IPA-aniline and acetone-water mixtures, which seemed to spread similarly to pure one-component liquids.

Of the alcohol-water mixtures, the methanol mixture differed from others in that the formed secondary droplets were larger in size at their initial formation. Similar behavior was observed for the IPA-glycerol mixture, in which the initial size of the secondary droplets was large enough that their formation process could be observed at the level of magnification used in the experiment. The formation process consists of the formation of a capillary ridge near the contact line, which then breaks up into droplets. The spreading of IPA-glycol mixture exhibited an instability that looked more like coarse "fingering" than droplet formation.

Series of images of the spreading of various mixtures are shown in Figs. 4.1-4.7.

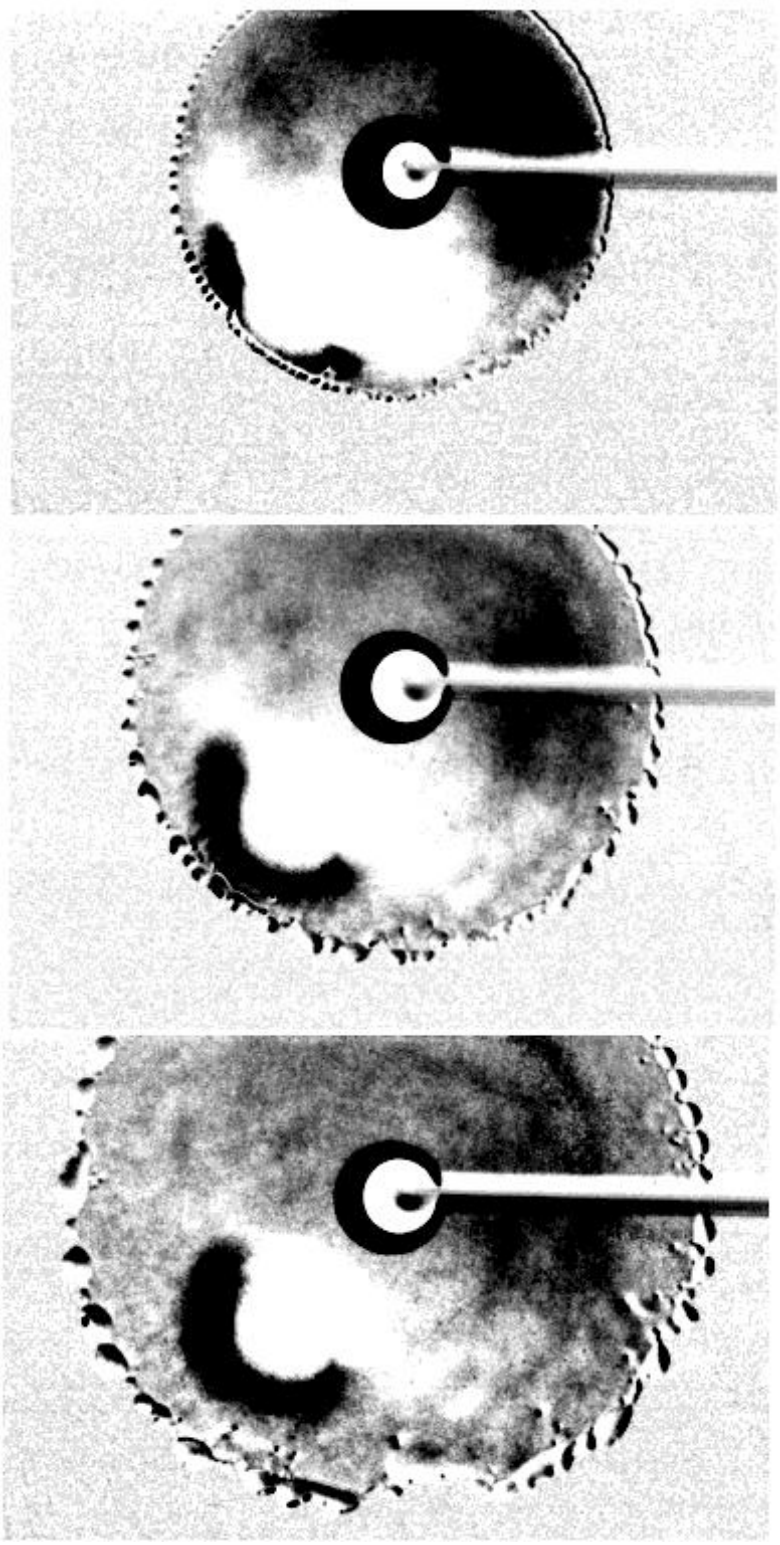

Figure 4.1: Spreading of a drop of 70% methanol solution on a glass slide.

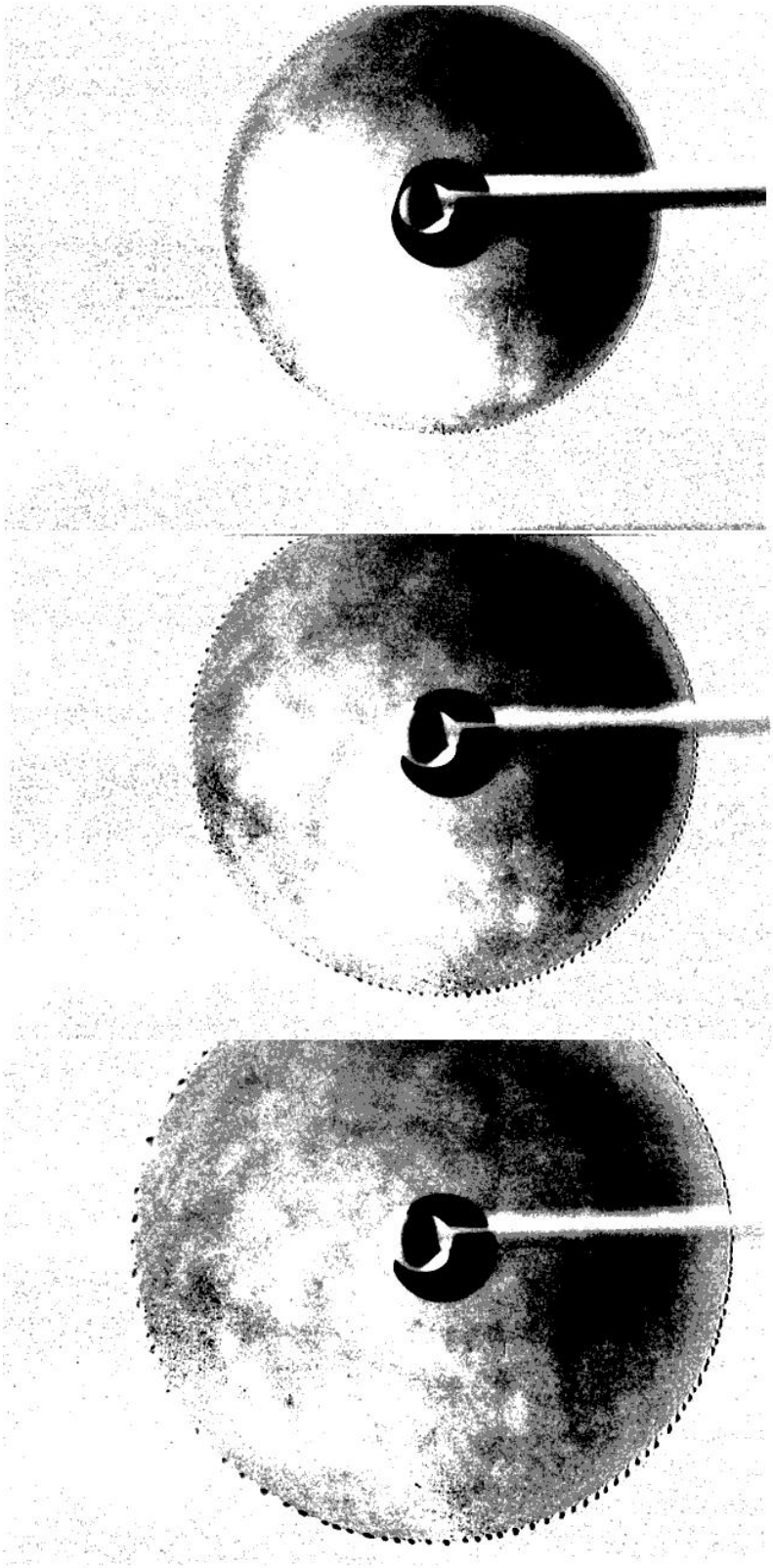

Figure 4.2: When a drop of 70% ethanol solution spreads on glass, a very symmetric ring of droplets appears at the expanding contact line.

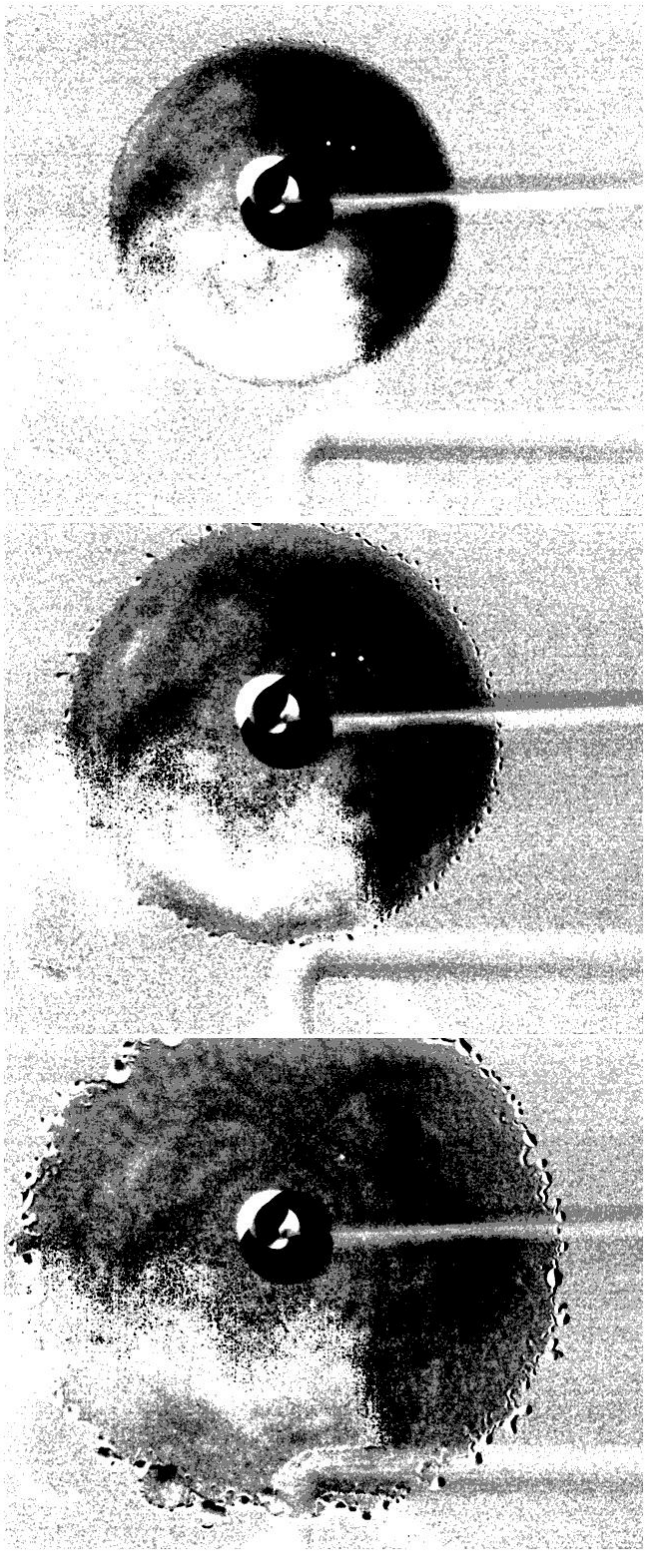

Figure 4.3: In spreading of a drop of 70% IPA, a more coarser and more unsymmetric ring of droplets is formed.

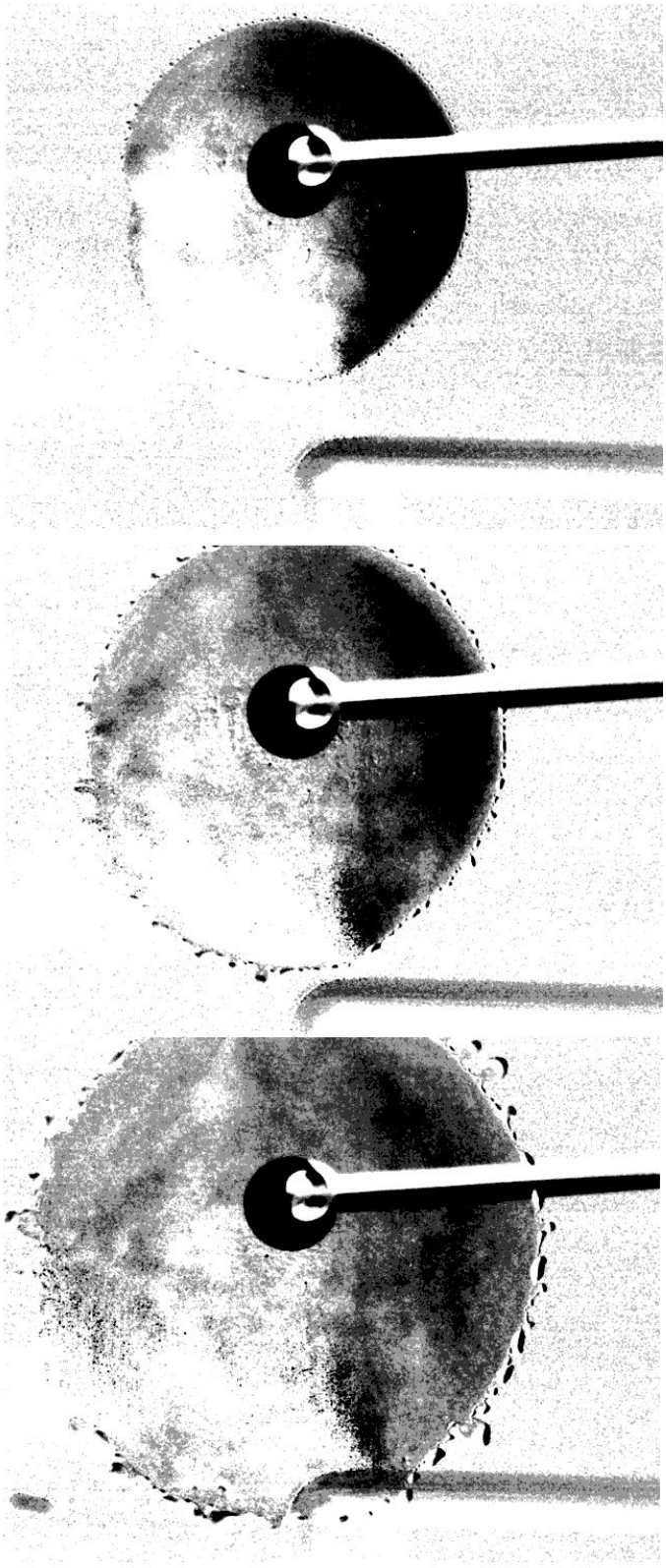

Figure 4.4: Spreading of a drop of 60% tert-butanol. At the end stage of spreading the contact line seems to form fingers with droplets at their tip.

Figure 4.5: In the spreading of a 70%/30% IPA-ethylene glycol mixture, a coarse fingering pattern is formed.

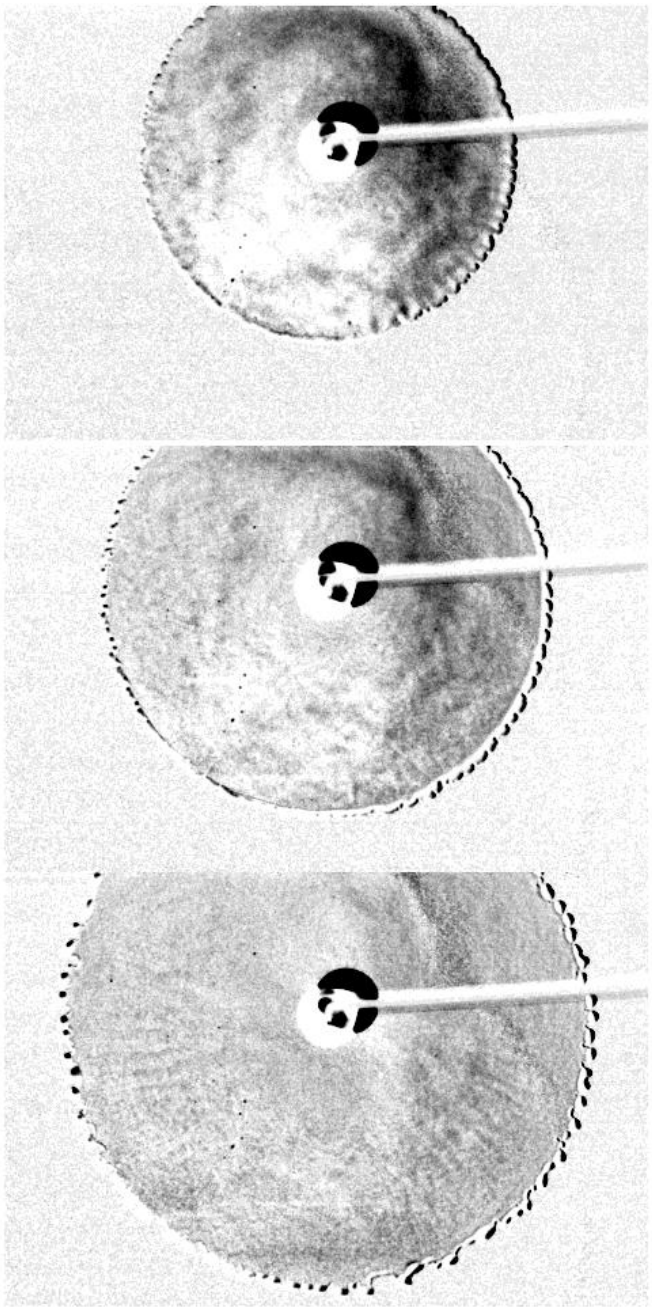

Figure 4.6: With the mixture of 20% glycerol in IPA, the droplet formation process happens at a larger length scale and is visible with the magnification used.

4.2 Spreading rates

To determine spreading rates, namely the exponent β in Tanner's power law, the diameter of the expanding liquid film was measured in pixels from about ten consecutive images taken with the high-speed camera. The data points were plotted with Origin Pro 8.5, and a function of the power law form $R(t) = A(t - t_0)^\beta$ was fitted in the results to determine the spreading exponent (A, t_0 and β are the fitting parameters). The actual scales of time and length in the plots, relative to seconds and millimeters, are not relevant, as they only affect the parameters A and t_0.

With the exception of the aniline mixture, which spreads similarly to a pure one-component fluid, all tested liquids spread with an exponent between 0.2 and 0.5. The spreading rate was at its maximum from the very beginning, unlike in the results of Cazabat et. al. in Fig. 3.3. One has to note that in the latest stages of evaporation, the liquid films start to contract back to smaller radius, because the volatile component has evaporated almost completely. All data points in these results are measured well before that contractile phase.

As can be seen from the results in Table 4.1, the mixtures with viscous liquids glycol and glycerol had a higher exponent, and the aniline mixture behaved almost like a pure liquid with $\beta \approx 1/10$.

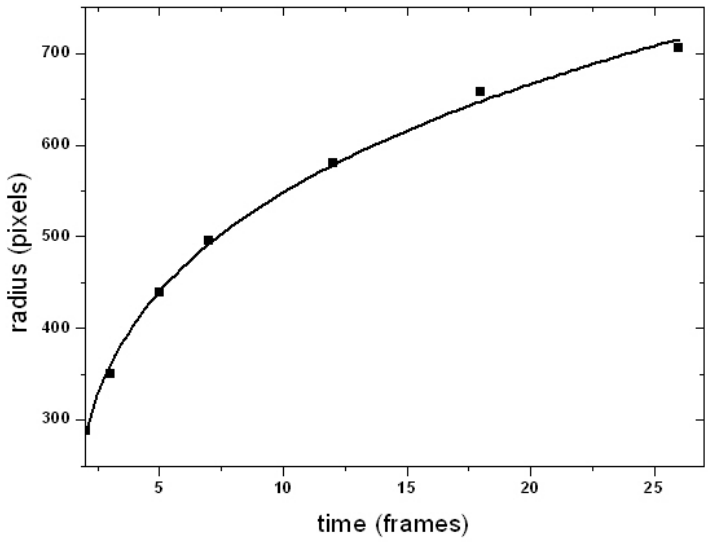

Figure 4.7: Radius of a spreading 70% methanol drop as a function of time, and a fit by a power-law.

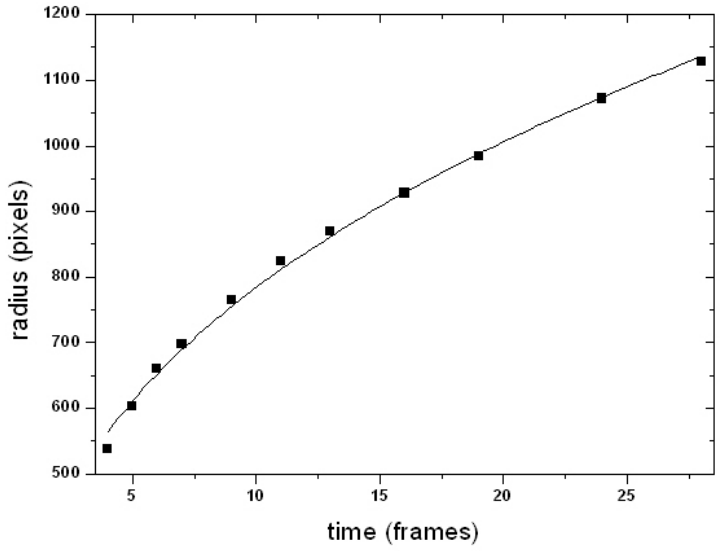

Figure 4.8: Radius of a spreading 70% ethanol drop as a function of time, and a fit by a power-law.

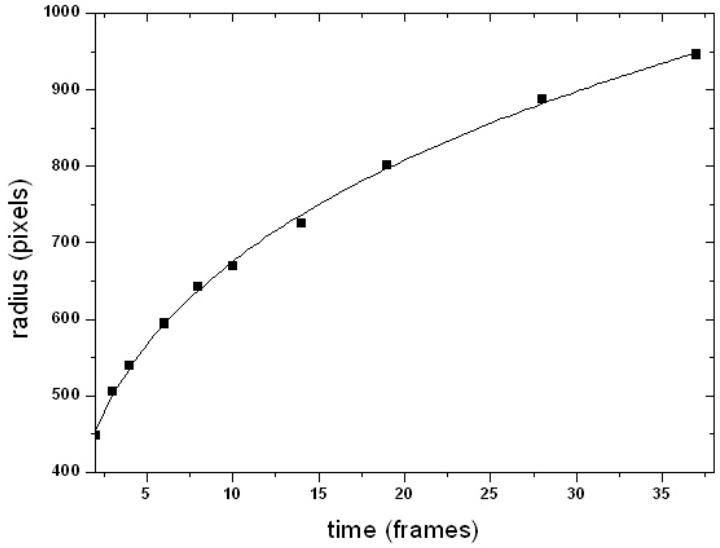

Figure 4.9: Radius of a spreading 70% isopropanol drop as a function of time, and a fit by a power-law.

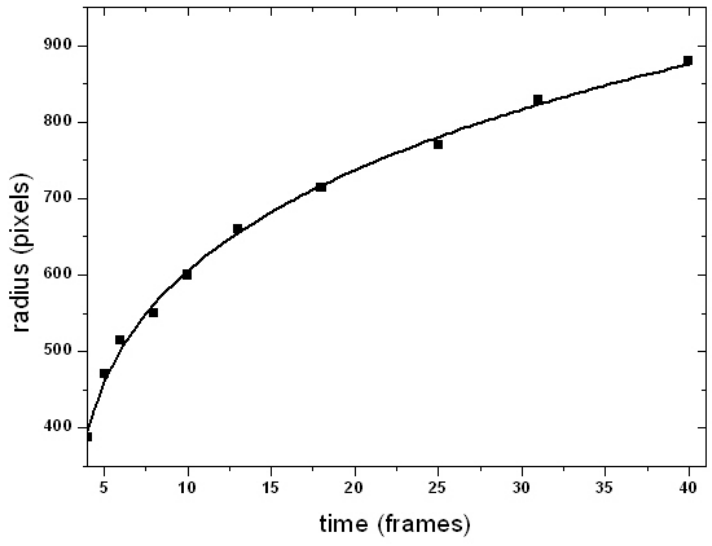

Figure 4.10: Radius of a spreading 60% tert-butanol drop as a function of time, and a fit by a power-law.

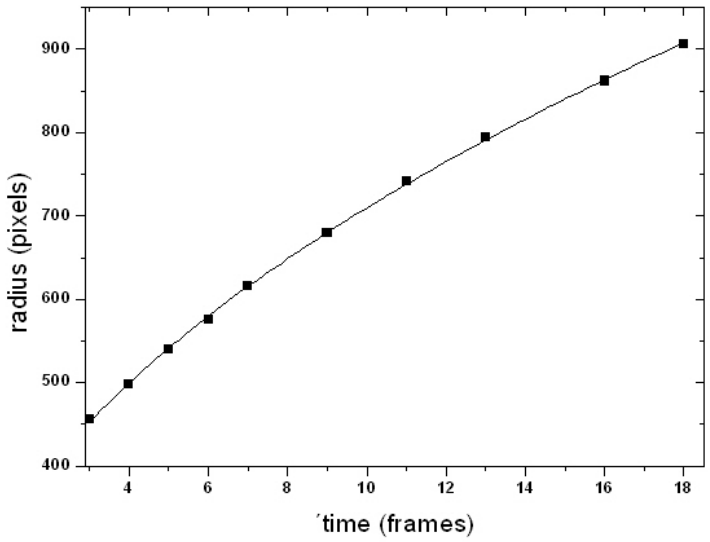

Figure 4.11: Radius of a spreading 70%/30% isopropanol/glycol drop as a function of time, and a fit by a power-law.

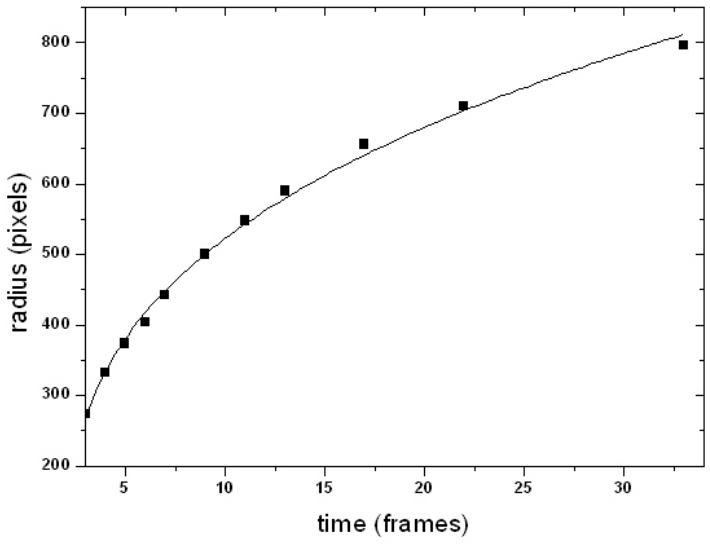

Figure 4.12: Radius of a spreading 80%/20% isopropanol/glycerol drop as a function of time, and a fit by a power-law.

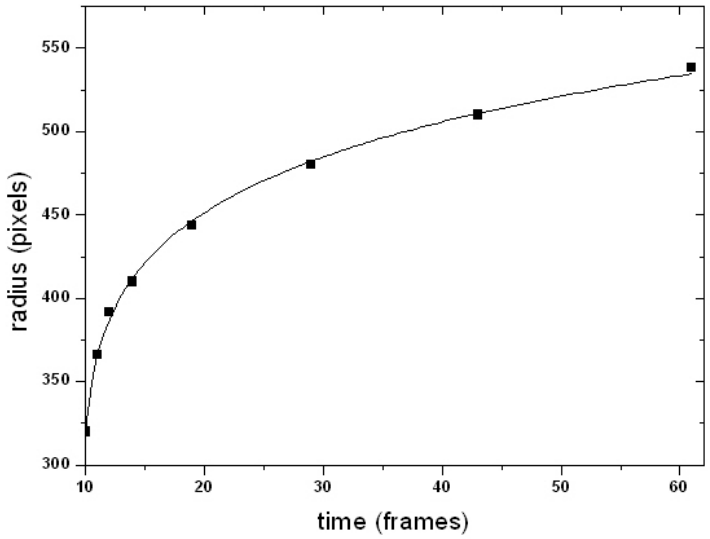

Figure 4.13: Radius of a spreading 70%/30% isopropanol/aniline drop as a function of time, and a fit by a power-law.

Table 4.1: The measured exponents in the power-law spreading of several mixtures.

Mixture	Exponent β
Methanol-Water	0.253 ± 0.014
Ethanol-Water	0.360 ± 0.008
IPA-Water	0.263 ± 0.010
TBA-Water	0.222 ± 0.010
IPA-Glycol	0.455 ± 0.014
IPA-Glycerol	0.324 ± 0.015
IPA-Aniline	0.105 ± 0.004

Chapter 5

Conclusions

The experimental results reported in this work demonstrate how a wide range of behaviors can be observed in systems where surface tension gradients affect the spreading of liquid films. Most of the studied mixtures consisting of components with significantly different surface tensions and volatilities exhibited unstable contact line behavior in their spreading on glass surfaces. The main differences were in how rapidly and in what size the secondary droplets formed at the vicinity of the contact line.

In the measurements, an anomalous finding was that the power-law exponent in the spreading of an ethanol solution is considerably larger than those for the spreading of other alcohol solutions. This is even more true for the mixtures of isopropanol with the viscous liquids glycol and glycerol. One could possibly hypothesize that the slower diffusion in more viscous mixtures makes the concentration gradients stronger (diffusion obviously tends to even out concentration differences).

For some reason the aniline-isopropanol mixture seemed to behave essentially similarly to pure one-component aniline. The spreading exponent (see Table 4.1) is close to the value 1/10 predicted by Tanner's law for pure nonvolatile liquid, and the spreading process does not exhibit instability similar to the alcohol-water mixtures. This fact is hard to explain without more measurements. One has to note, though, that despite its relatively high surface tension, aniline seems to have a very small equilibrium contact angle on glass surface. It could also be possible that aniline reacts with isopropanol by some nucleophilic substitution mechanism, distorting the results.

The acetone-water mixture did not behave in a manner similar to alcohol solutions and did not form secondary droplets at the expanding contact line, which is a somewhat puzzling observation. One possible explanation to this is that the high volatility of acetone makes the "instability wavelenght" comparable to or larger than

the circumference of the expanding drop, making it impossible to observe the instability. This seems logical, noting that the solution of methanol, the most volatile alcohol, formed considerably larger droplets that other alcohol solutions. However, one article ([24]) describes an instability in the spreading of a ternary water-acetone-glycerol mixture.

A curious fact is that even though the surface tension differences between the components in our mixtures are at least ten times larger than the corresponding differences in binary alkane mixtures, the spreading exponents we measured were not that different compared to those measured in the work by Cazabat *et. al.* on alkanes (see Section 3.2).

The experimental setup used in this work could give rise to several sources of error. Usually the glass slides used in spreading experiments are pretreated with nitric acid or piranha solution (mixture of sulphuric acid and hydrogen peroxide) to remove impurities, and then kept in a hot oven for several hours to eliminate moisture. In our work such measures were not taken. Another source of error could be atmospheric humidity. Concentrated alcohol solutions are hygroscopic (absorb moisture from air), and that could affect the results. In more sophisticated work, the measurements should probably be made in an enclosed atmosphere of dry nitrogen, and also possibly in clean-room conditions.

Bibliography

[1] N. Fraysse, G. M. Homsy, "An experimental study of rivulet instabilities in centrifugal spin coating of viscous Newtonian and non-Newtonian fluids", Phys. Fluids., 6, 1491 (1994).

[2] E. Pauliac-Vaujour, A. Stannard, C. P. Martin, M. O. Blunt, I. Notingher, and P. J. Moriarty, "Fingering instabilities in dewetting nanofluids", Phys. Rev. Lett., 100, 176102 (2008).

[3] F. White, "Fluid Mechanics", McGraw Hill, 4th ed.

[4] A. Oron, S. H. Davis, S. G. Bankoff, "Long-scale evolution of thin liquid films", Rev. Mod. Phys., 69, 931-980 (1997).

[5] H. Knüpfer, "Classical solutions for a thin-film equation", PhD thesis, University of Bonn.

[6] A. L. Bertozzi, "The mathematics of moving contact lines in thin liquid films", Notices Am. Math. Soc., 45, 689-697 (1998).

[7] S. Rafai, D. Bonn, A. Boudaoud, "Spreading of non-Newtonian fluids on hydrophilic surfaces", J. Fluid Mech., 513, 7785 (2004).

[8] J. A. Diez, L. Kondic, "Computing Three-Dimensional Thin Film Flows Including Contact Lines", Journal of Computational Physics, 183, 274-306 (2002).

[9] F. Bernis, J. Hulshof, J. R. King, "Dipoles and similarity solutions of the thin film equation in the half-line", Nonlinearity, 13, 413439 (2000).

[10] R. Ferreire, F. Bernis, "Source type solutions to thin film equations in higher dimensions", European Journal of Applied Mathematics, 8, 507-524 (1997).

[11] E. Sultan, A. Boudaoud, M. B. Amar, "Evaporation of a thin film: diffusion of the vapour and Marangoni instabilities", J. Fluid Mech., 543, 183-202 (2005).

[12] N. Tiwari, J. M. Davis, "Stability of a volatile liquid film spreading along a heterogeneously-heated substrate", J Colloid Interface Sci., 355, 243-251 (2011).

[13] U. Thiele, K. Neuffer, Y. Pomeau, M. G. Velarde, "On the importance of nucleation solutions for the rupture of thin liquid films", Colloids and Surfaces A: Physicochemical and Engineering Aspects, 206, 135155 (2002).

[14] W. H. Press, S. A. Teukolsky,W. T. Vetterling, B. P. Flannery, "Numerical Recipes in C", Cambridge University Press, Cambridge, 2nd ed., 2002.

[15] E. Momoniat, C. Harley, E. Adlem, "Numerical investigation of the generalized lubrication equation", Applied Mathematics and Computation, 217, 26312638 (2010).

[16] J. D. Jackson, "Classical Electrodynamics", 1st ed. Wiley, New York, 1962.

[17] R. D. Deegan, O. Bakajin, T. F. Dupont, G. Huber, S. R. Nagel, and T. A. Witten, "Contact line deposits in an evaporating drop", Phy. Rev. E, 62, 756 (2000).

[18] L. Kondic, "Instabilities in Gravity Driven Flow of Thin Fluid Films", SIAM Review, 45, 95-115 (2003).

[19] L. W. Schwartz, R. V. Roy, R. R. Eley and S. Petrash, "Dewetting Patterns in a Drying Liquid Film", Journal of Colloid and Interface Science, 234, 363374 (2001).

[20] M. Iwamatsu, "The characterization of wettability of substrates by liquid nanodrops", Colloids and Surfaces A: Physicochemical and Engineering Aspects, 420, 109114 (2013).

[21] N. Murisic and L. Kondic, "Octopus-shaped instabilities of evaporating drops", Proc. Appl. Math. Mech., 7, 21000392100040 (2007).

[22] N. Murisic, "Instabilities of volatile films and drops", PhD thesis, New Jersey Institute of Technology.

[23] A. M. Cazabat, G. Guena, C. Poulard, "Evaporating drops of alkane mixtures", Colloids and Surfaces A: Physicochem. Eng. Aspects, 298, 211 (2007).

[24] D. W. Mundell, "Marangoni Flowers and the Evil Eye: Overhead Presentations of Marangoni Flow", Journal of Chemical Education, 86, 833 (2009).